The rotating stator concept preliminary calibration of the compressor in the conventional configuration

Chappell, M. S.

Publisher's version / Version de l'éditeur:
https://doi.org/10.4224/40003749
Mechanical Engineering Report (National Research Council Canada. Division of Mechanical Engineering. Engine Laboratory); no. ME-234, 1970-07

NATIONAL RESEARCH COUNCIL OF CANADA

MECHANICAL ENGINEERING REPORT
ME-234

THE ROTATING STATOR CONCEPT
PRELIMINARY CALIBRATION OF THE COMPRESSOR IN THE CONVENTIONAL CONFIGURATION

by

M. S. CHAPPELL

DIVISION OF MECHANICAL ENGINEERING

OTTAWA

JULY 1970

NRC NO. 11841

THE ROTATING STATOR CONCEPT
PRELIMINARY CALIBRATION OF THE COMPRESSOR IN THE CONVENTIONAL CONFIGURATION

by

M. S. CHAPPELL

E. P. Cockshutt, Head
Engine Section

D. C. MacPhail
Director

SUMMARY

The background and objectives of an extensive program of research into a novel concept of co-rotating stator rows within an axial compressor are outlined. The test compressor to be used in the experimental investigations is described in detail, as is the NRC Compressor Test Facility wherein the tests are conducted.

The major portion of this initial report comprises results from the preliminary calibration of the three-stage test compressor operated in the conventional configuration (i.e. with the stator rows stationary). This datum performance run was prematurely terminated by a drive train failure but some useful data were obtained at speeds up to about eighty percent of the design value. These data are compared with results from a previous series of tests on another compressor of the same aerodynamic design. The correlation of overall performance parameters was acceptable, but individual stage characteristics required considerable adjustment to obtain satisfactory agreement with previous results.

TABLE OF CONTENTS (Cont'd)

TABLES

APPENDICES

ILLUSTRATIONS

ILLUSTRATIONS (Cont'd)

ILLUSTRATIONS (Cont'd)

SYMBOLS

Symbol	Definition	Units
A	Area	in^2
Cp	Specific heat at constant pressure	$CHU/lb_m°K$
g_o	Dimensional constant	$32.174 \frac{lb_m}{lb_f} \frac{ft}{sec^2}$
h	Specific enthalpy	$\frac{CHU}{lb_m}$
J	Dimensional constant	$1400.71 \frac{ft\ lb_f}{CHU}$
K_p	Dimensional constant ($K_p \equiv g_o JCp$)	$\frac{ft^2}{sec^2 °K}$
le	Leading edge	-
$\dot{m}$	Mass flowrate	lb_m/sec
N	Rotational speed	rpm
P	Total pressure	psia, $"Hg_{abs}$
p	Static pressure	psia, $"Hg_{abs}$
PR	Pressure ratio	-
R	Rotor (e. g. 4R denotes Stage 4 rotors)	-
S	Stator (e. g. 3S denotes Stage 3 stators)	-
T	Total temperature	°K
te	Trailing edge	-
ΔT_C	Increase of total temperature through entire compressor	°K

Symbol	Definition	Units
ΔT_{ST}	Increase of total temperature across one stage	°K
U_T	Tip speed (based on 3R le diameter of 14.999")	ft/sec
U_M	Blade midspan peripheral velocity	ft/sec
V_A	Axial velocity	ft/sec
X	Axial distance measured in flow direction from 3R le	in
δ	Total pressure correction factor $\left(\delta \equiv \frac{P_{IN}\ (\text{"Hg}_{abs})}{29.92}\right)$	-
ϕ	Flow coefficient $\left(\phi \equiv \frac{V_A}{U_M}\right)$	-
η_{CT}	Compressor adiabatic efficiency based on temperature and pressure rise measurements $\left(\eta_{CT} \equiv \frac{(\Delta h_C)_{isentropic}}{(\Delta h_C)_{actual}} \approx \frac{(\Delta T_C)_{isentropic}}{(\Delta T_C)_{actual}}\right)$	-
η_{ST}	Stage adiabatic efficiency $\left(\eta_{ST} \equiv \frac{(\Delta h_{ST})_{isentropic}}{(\Delta h_{ST})_{actual}} \approx \frac{(\Delta T_{ST})_{isentropic}}{(\Delta T_{ST})_{actual}}\right)$	-
ψ	Work coefficient $(\psi \equiv \eta_{ST}\ K_p\ \Delta T_{ST} / U_M^2)$	-
θ	Total temperature correction factor $\left(\theta \equiv \frac{T_{IN}}{288.16}\right)$	-

THE ROTATING STATOR CONCEPT
PRELIMINARY CALIBRATION OF THE COMPRESSOR
IN THE CONVENTIONAL CONFIGURATION

1.0 INTRODUCTION

The Small Compressor Program is a co-operative project between the National Research Council of Canada (NRC) and Rolls-Royce (Canada) Limited (RR). Its objectives are to investigate, both analytically and experimentally, the Fanstat principle of compressor spooling. This concept envisions driving the fan of a turbofan engine by permitting co-rotation of both rotor and stator rows in the axial compressor of the core engine. The fan blades would be mounted on the rotating stator casing. The primary function of the Fanstat is to provide an "aerodynamic gearbox" that will permit both the fan and the fan turbine to operate more closely to their individual optimum speeds. It is thus an attempt to overcome the rotational speed mismatch inherent in high bypass-ratio turbofan engines.

This report describes the basic test compressor and the experimental facilities used, together with the test results obtained during the initial calibration of the test compressor in its conventional configuration. These results are compared with analytic and experimental data obtained by Rolls-Royce during their tests on an aerodynamically-identical compressor.

1.1 Choice of Test Compressor

The test vehicle used for the first series of experiments was chosen from various existing compressor designs. It comprised the rear three stages of the five-stage "V-2" axial compressor designed by Rolls Royce under contract from the United Kingdom Ministry of Technology. Major factors leading to the choice of this compressor were:

a) It was of appropriate size for testing in the NRC Variable Density Compressor Test Facility.

b) It comprised free vortex blading with an aerodynamic loading typical of current design practice.

c) By selecting only the last few stages of a multistage compressor, rotational speed was significantly reduced while maintaining the design value of $N/\sqrt{T}$ at entry to the first rotating row. Thus, mechanical limitations such as blade stress and tip growth permitted significant stator case peripheral velocities at full relative (rotor vs stator) speed.

d) Complete aerodynamic design data were available for "V-2, Stages 3 to 5" from British Ministry and Rolls Royce files, together with some tooling and fixtures for assembly of the high speed rotor.

e) "V-2, Stages 3 to 5" had been tested by Rolls Royce in England and therefore considerable previous data and experience were available for comparison with the NRC-generated results.

The initial configuration of the core compressor (see Fig. 1 and A-2) comprised Stages 3, 4, and 5 of V-2 blading without inlet guide vanes. The rotor blades were assembled using NRC-designed front and rear shafts and RR-designed interstage discs. The stator rows comprised RR-designed airfoil sections set onto NRC-designed platforms. The Engine Laboratory, NRC, also undertook the design of all additional rows of blading required to convert the conventional V-2 compressor into the Fanstat configuration, the design of all mechanical components, instrumentation, and service systems. The interstage discs and V-2 blading rows were manufactured in the Rolls Royce plant at Barnoldswick, England. All other components were manufactured in the Experimental Workshops of the NRC.

1.2 Experimental Program Synopsis

The Small Compressor Program has been subdivided into several phases as described in the following paragraphs.

1.2.1 Phase Zero

This Phase constitutes a standard compressor test of "V-2, Stages 3 to 5". The stator casing is stationary at all times and the results form the basic reference for subsequent comparison with results from later phases. A secondary comparison is also made with data recorded previously by Rolls Royce during their tests on "V-2, Stages 3 to 5".

1.2.2 Phase One

Structural considerations, associated with mounting the rear of the rotating stator case for Phase Two on the fifth-stage stators, dictated a significant increase in the cross-sectional area of these blades. Phase One is, therefore, merely a repeat of Phase Zero with the so-called "long chord fifth-stage stators" instead of the standard fifth-stage stators originally designed for the V-2 compressor. The new stators were designed using the same method as that used in the original design and, moreover, the pitch:chord ratio was maintained at the original value. Consequently, the performance differences between Phases Zero and One are expected to be small. However, the mechanical configuration of the Phase One unit is closely related to that of Phase Two.

1.2.3 Phase Two

This phase incorporates rotation of the stator casing whilst restrained by a water-brake dynamometer instead of a fan. This arrangement permits independent variation of the fan speed and fan torque, thus yielding results over a wider range of operating conditions than would be possible with a fixed geometry fan and its unique running line.

This phase explores the basic performance of the Fanstat principle and therefore is considered to be the most significant portion of the test program.

1.2.4 Subsequent Investigations

Based on the results of Phase Two, a fan could be designed to match the power output characteristics of the rotating stator case. Phase Three might therefore

test a hardware configuration of the Fanstat concept in a form that could represent an actual engine application. It would be primarily concerned with the transient performance of both the fan and the core compressor, especially when one or both of these components were operating at or near their surge lines.

2.0 TEST FACILITY

2.1 Variable Density Tunnel and Drive System

The experimental testing for all phases of the Small Compressor Program is conducted in the Variable Density Compressor Test Facility in the Gas Dynamics Laboratory of the National Research Council. Figure 2 illustrates this facility, and Table I lists its major specifications and capacities.

The drive system arrangement used during the Phase Zero tests comprised: a two-stage axial turbine, a 1.946:1 speed-increasing gearbox, a dummy torqueshaft, and various sections of shafting connected to the test unit in the working section. The drive turbine was fed with compressed air from a large centrifugal plant compressor located in the same machinery bay as the Compressor Test Facility. Control of turbine speed (and hence test compressor speed) was achieved by throttling the intake to the plant compressor and by simultaneous blowing-off from a connection in the line feeding the rig drive turbine. Approximately three minutes were required to change from one steady speed to another, or to re-establish the speed setting after adjusting the test compressor back-pressure. Once stable conditions had been reached, however, speed could be held to about ±0.2% throughout the data-recording period.

Although the tunnel is designed for closed circuit operation, and indeed can be partially evacuated, the Phase Zero testing was performed with the top half of the split working section removed. Hence, the test compressor inlet pressure was substantially atmospheric.

2.2 Control Rooms and Rig Instrumentation

The control room for the plant compressor is located above the north end of the machinery bay and is connected to the test facility observation room by an intercom system. A digital readout of test compressor speed is provided in the control room so that the plant compressor operator can establish and maintain steady the speed demanded by the test engineer via the intercom system from the tunnel observation room. A small, remotely operated trimming valve in the turbine feed line can be actuated directly from the tunnel observation room for fine speed control.

The observation room for the drive system and the test compressor is located on the east side of the tunnel, approximately opposite the working section, and is elevated about four feet from the operating floor level (see Fig. 2). For Phase Zero of the Small Compressor Program, the readout instrumentation was divided into four main areas, as shown in Figure 3.

2.2.1 Drive System Control Panel

This area contained speed, vibration, and bearing temperature instrumentation for all components in the drive train up to the intermediate shaft next to the test compressor itself. Automatic shutdown relays were connected to speed, vibration,

TABLE I

VARIABLE DENSITY COMPRESSOR TEST FACILITY

SPECIFICATIONS AND CAPACITIES

AIR CIRCUIT DATA

Total Length of Circuit Centerline	81.3	feet
Length of Working Section	4.33	feet
Diameter of Working Section	53.63	inches
Width of Working Section between Mounting Shelves	47.75	inches
Diameter of Venturi Throat	23.194	inches
Pressure Limits (Structural)		
Minimum Compressor Inlet Pressure	1/2	atm
Maximum Compressor Outlet Pressure	6	atm
Grate Valve Opening: Maximum (Nominal)	full	
Minimum (Nominal)	zero	
Cooler Capacity: at 15°C Compressor Inlet Temp.	2000	CHU/sec

DRIVE SYSTEM DATA

	HOT	COLD	
Power Available: 100% Speed	4500	2500	hp
Rated Maximum Speed of Turbine	20,000		rpm
Gearbox Ratios Available (Nominal) a) 1.0:1			
b) 1.5:1			
c) 2.0:1			

and all bearing temperature signals. A manually operable Emergency Shutdown Button, which vented the drive turbine air supply to atmosphere, was also provided. Torquemeter readout instruments will be installed in this panel in the future.

When in use, the tunnel "grate valve" (Fig. 2) is controlled by a linear hydraulic transmitter-receiver system whose sending unit is located below the observation room window between the drive system control panel and its associated manometer boards. For all phases of the Small Compressor Program, this valve is locked in the fully open position and test compressor back-pressure is regulated by a throttle valve in the test compressor outlet annulus (see Fig. 4).

2.2.2 Test Compressor Control Panel

Mechanical parameters similar to those in 2.2.1 were displayed for the test compressor unit on this panel, together with test unit lubrication system temperatures and pressures. All bearing temperatures were monitored on separate instruments. No automatic shutdown relays were provided on this panel, but the operator was within reach of the Emergency Shutdown Button on the drive system console.

The controls and position indicator for the test compressor efflux throttle were also located on this panel, together with a single-tube manometer reading outlet static pressure that was used to determine the proper setting for this efflux valve. The jacking screws that positioned the conical throttle valve were chain-driven from a high-torque reversible dc motor mounted outside the tunnel. The actuating circuits were arranged to permit slow "inching" control while closing the valve, and a quick-opening mode to rapidly relieve the back-pressure on the test compressor during investigations at the surge line. Limit switches were set to give a final exit area (see A* in Fig. 4) between 30% and 150% of the compressor exit annulus (diffuser entry) area.

2.2.3 Test Compressor Manometer Boards

Seven ten-tube manometer boards were provided for measuring various aerodynamic pressures throughout the test compressor. These instruments were arranged along the east wall of the observation room as shown in Figure 3. The two 40-inch banks were equipped with individual wells for each tube, whereas the 70-inch and 100-inch banks were furnished with infinitely adjustable common wells. It was therefore possible to utilize only nine out of ten tubes on these latter two sizes of instrument, the tenth being required to indicate the datum or well fluid level.

All sixty-five active manometer tubes are permanently connected to bulkhead fittings on the instrumentation hatch covers at the east side of the tunnel working section.

2.2.4 Test Compressor Performance Panel

This panel comprises two pairs of standard instrumentation racks pivoted about a central column to provide ready access to the back connections of the instruments. These racks are available for all test unit performance instrumentation required in addition to the manometer boards described in 2.2.3 above. Typically, aerodynamic temperature readout, probe controllers, scanivalve controllers, and automatic data logging equipment can be installed in this location. Forty-eight cold-junction-compensated iron-constantan thermocouples are permanently wired from a self-balancing potentiometer in this panel to a junction box on the east side of the tunnel working section.

3.0 CONFIGURATION OF TEST COMPRESSOR FOR PHASE ZERO

3.1 Aerodynamic Configuration

As outlined in Section 1.2, the Small Compressor Program comprises a series of comparative tests, and therefore it is necessary to preserve as much similarity as possible in the test equipment used for the various phases. By so doing, extraneous differences can be minimized, and a clearer comparison obtained of the true effects of the independent test parameters. Phase Two of the program requires a dynamometer, mounted in the tunnel upstream of the compressor, to restrain the rotating stator case. In order to establish the same entry configuration for all phases, the fairings for the dynamometer and connecting shaft were installed in the tunnel prior to Phase Zero. Figure A-1 presents the geometry of the compressor intake airpath (see also Section 6.1.2).

Compressor annulus dimensions and blading specifications were identical with the Rolls Royce designed "V-2, Stages 3 to 5". Moreover, to avoid confusion between the two organizations, the three stages of the NRC test vehicle were called 3, 4, and 5; i.e. the same nomenclature as used for the Rolls Royce components. Airfoil and annulus data are summarized in Appendix A.

The outlet diffuser extended rearward 11.75 inches from the end of the parallel exit annulus at station V on the diagram of Figure A-2. The annulus area increased by 60% from 44.85 square inches to 71.71 square inches in this length, giving a 3-1/2° half-angle on the inner wall; the outer wall was cylindrical.

The diffuser inner wall terminated in a short cylindrical extension on which the back-pressure control valve fitted, as shown in Figure 4.

3.2 Mechanical Configuration

The general mechanical arrangement of the Phase Zero apparatus is shown in Figure 1. It comprised three main elements, viz: the intermediate shaft, a flexible gear-coupling, and the test compressor itself. In order to obtain a significant proportion of parts that could be used throughout all phases of the program, the mechanical arrangement of the Phase Zero compressor incorporated many Phase Two components with adaptors (e.g. dummy bearings) for the preliminary configuration. Thus the assembly shown in Figure 1 appears much more complex than would be expected for a simple three-stage axial compressor.

The intermediate shaft served as part of the connection between the rig drive and the experimental apparatus. It was axially located by a deep groove angular contact ball bearing at the forward end. A roller bearing provided radial location at the power input end. Each of these two bearings was jet-lubricated by about 10 IGPH of synthetic turbine oil supplied at 50 psig through two 0.030-inch orifices. This oil supply was taken from the main system used for all driveline components and, therefore, was independent of the lubrication system used for the test compressor itself. Positive scavenging at about 1-1/2 inches mercury suction was provided by a vane pump that returned the hot oil, via a heat exchanger, to the main tank.

The gear-coupling provided a flexible connection between the intermediate shaft and the test compressor, both of which were rigidly fastened to the variable density tunnel structure. The barrelled involute gear tooth couplings at each end of this component were lubricated with semi-fluid grease, which was loaded into the hollow shaft on assembly.

The compressor rotor was supported between ball and roller bearings. The aft split-inner-race ball bearing was supplied by Rolls Royce and provided axial location for the compressor rotor as well as accommodating the 1900-lb_f forward thrust of the rotor. The forward end of the rotor was carried in a roller bearing identical with that used in the aft end of the intermediate shaft. Both compressor bearings were jet-lubricated with synthetic turbine oil at approximately 40 IGPH and 10 IGPH for the ball and roller bearings, respectively. Orifice diameters were 0.052 and 0.030 inch, and two jets at about 60 psig were aimed at the inner race contact line of each bearing. Positive scavenge at about 10 inches mercury suction removed the oil from the bearing cavities and returned it via a cooler to the reservoir tank.

Instrumentation was provided to monitor oil temperatures and pressures throughout the lubrication system. Thermocouples spring-loaded against the outer race of each bearing were connected to separate readout instruments so that the operator could simultaneously monitor all four bearing temperatures.

Leakage of hot compressor efflux and ambient air into the bearing scavenge cavities was minimized by fitting labyrinth seals between rotating and stationary components adjacent to the air annulus, and by fitting controlled gap carbon seals adjacent to the scavenge cavities. Leakage past the labyrinth seals was collected in manifolds and piped rearward through two venturis into the vicinity of the choke valve exit. Measurement of this leakage mass flow was necessary as this amount of air had undergone the full compression process and had therefore to be taken into account when computing performance characteristics.

Vibration was monitored in the vertical plane at three axial locations. Front and rear compressor locations were fitted with piesoelectric accelerometers mounted within the apparatus immediately adjacent to the bearing housings. In addition, electromagnetic accelerometers were mounted on the front and rear of the compressor main mounting frame, as well as on the hub of the intermediate shaft (see Fig. 1).

3.3 Performance Instrumentation

Instrumentation for assessing the performance of the Phase Zero compressor comprised four groups. These groups are described in the following sub-paragraphs, and Reference 3 details the type of readout devices used.

3.3.1 Inlet Instrumentation

Inlet conditions were assessed at a plane approximately 1/2 inch forward of the leading edges of the intake struts (Fig. 5). Sixteen separate thermocouples in kiel probe shrouds measured inlet total temperature at the mid-radii of four concentric annulae of equal area on each of four intake struts. These were connected to pushbutton switches on a self-balancing potentiometer in such a way as to permit

simultaneous selection of groups of four thermocouples that gave circumferential average temperatures for each of the four radial positions. Individual thermocouples could also be selected to check proper functioning and to confirm the average values obtained using the technique described above.

Intake total pressure was measured by sixteen probes disposed on the intervening four intake struts in the same equal-area radial positions as the thermocouples. Manifolds provided permanent circumferential averaging, and readout was on four water manometers - one for each radial position.

Inner-wall and outer-wall static pressure tappings were provided at 90° intervals around both peripheries and were indicated on two other water manometers.

3.3.2 Outlet Instrumentation

In general the outlet instrumentation was arranged in a similar manner to the inlet instrumentation, except that the total temperature probes were displaced rearward to reduce blockage in this smaller annulus (Fig. 6). Twenty thermocouples were used at five radial locations on each of four probe-support struts. Again, selector switches were arranged to give four-point circumferential averages or individual readouts.

Only three total pressure probes were used at each of the four circumferential positions and these were manifolded to give a circumferential average for each of the three radial positions. Readout was on three 100-inch mercury manometers.

Inner-wall and outer-wall static tappings were arranged at 90° intervals as for the inlet, and these were also displayed on 100-inch mercury manometers. In addition, the outer-wall static pressure was displayed on another mercury manometer adjacent to the efflux throttle controls as a convenience in setting the desired outlet pressure (see Sect. 2.2.2).

3.3.3 Interstage Static Pressures

Outer-wall static tappings were located between each blade row as shown in Figure 7. Three tappings, midway between blade wakes, were provided at each axial station and manifolded to give an average static pressure at each interstage location. All seven measurements were displayed on separate 100-inch mercury manometers.

A single traversable wedge probe was located approximately 2-1/2 inches downstream from the trailing edges of the fifth-stage stators (near the leading edges of the small uncambered vanes that are replaced by the stationary outlet guide vanes for Phase Two). Traversing gear automatically positioned the probe at any one of the four penetrations shown in Figure 7. The probe could also be yawed or rotated remotely to null the two sideface statics, thus aligning the wedge to the outlet flow direction. Angular position (from the axial), total temperature, and total and static pressures were then recorded.

3.3.4 Miscellaneous Performance Instrumentation

Other performance data were recorded as indicated on the sample Data Sheets in Reference 3. Brief descriptions of the major items are given below.

Rotational Speed: A toothed wheel was mounted on the free end of the turbine shaft. Magnetic proximity pickups fed pulses into a digital counter whose time base had been adjusted to account for the speed-increasing gearbox (1.945:1) in the drive train. The counter displayed compressor rpm divided by ten.

Leakage Air: As mentioned in Section 3.2, the leakage air was discharged through two venturis (for space reasons only). Upstream and throat tappings from both venturis were read on 40-inch manometers. Metal and efflux air temperatures were allocated switch positions on the self-balancing potentiometer.

Atmospheric Air Pressure: An aneroid barometer calibrated to ±0.5 mb was mounted in the Compressor Control Room.

4.0 TEST PROCEDURE

After a period of preliminary running to overcome various mechanical difficulties with the new facility and drive system, testing along lines of constant corrected speed commenced. The test compressor was accelerated from standstill along a prescribed speed back-pressure curve known as the Safe Acceleration Line (SAL). This curve had been established by previous testing at Rolls Royce, Derby, and was merely an operating line that lay well away from both choke and surge lines.

The compressor was operated on the SAL at approximately the desired speed until the rig temperatures had stabilized, and then the speed was adjusted to the precise corrected value based on an average measured inlet temperature. One datum point was recorded at this condition. One or two additional data points were then taken at higher pressure ratios along the constant corrected speed line as back-pressure was increased towards the surge point.

In order to establish the surge point on each constant speed characteristic, the efflux throttle valve was gradually closed until a sharp drop in outlet static pressure was observed. This was usually accompanied by a distinct change in compressor noise and a rapid increase in speed as the unit unloaded aerodynamically. Outlet static and total pressures, and outlet total temperature (mid-annulus positions) were monitored constantly as surge was approached. The maximum values were recorded as the surge point. This procedure was repeated once to confirm the initial observations.

Immediately following establishment of the surge point, a complete set of steady-state data were recorded at a pressure ratio just below the surge value. Other steady-state data points were then taken along the constant corrected speed line at pressure ratios decreasing towards the choking value. This particular compressor

did not exhibit any marked change of characteristics at the choking point, so data were recorded at lower and lower pressure ratios until the intake static pressure no longer decreased with decreasing back-pressure.

It was intended that the following constant speed characteristics be delineated.

TABLE II

ROTATIONAL AND TIP SPEEDS AS PERCENTAGES OF DESIGN POINT VALUE

$\%(N/\sqrt{\theta})$	56.3%	64.4%	72.4%	80.5%	88.5%	96.5%	100%	104.6%
$N/\sqrt{\theta}$ rpm	10696	12224	13752	15280	16808	18336	18993	19864
$U_T/\sqrt{\theta}$ ft/sec	700	800	900	1000	1100	1200	1243	1300

However, bearing problems in both the drive train and the test compressor prevented running in excess of about 17,000 rpm. Indeed, a major failure of the dummy torque-shaft forced a premature halt to testing, and few useful data were obtained at or above the 88.5% (1100 ft/sec) characteristic line.

5.0 DATA REDUCTION ROUTINE

The data reduction computer program used to derive both overall and stage characteristics from the experimental observations is described in detail in Reference 3. The following paragraphs outline the major portions of the calculation procedure, and Appendix B contains a sample of the output sheets.

5.1 Overall Compressor Performance

The following steps were used to compute the overall compressor performance parameters.

1. Average inlet total temperature and average inlet total pressure were computed from the four recorded values of each variable, each one being a circumferential average of four points on the same radius. These average values were used to establish intake temperature and pressure correction factors (θ and δ) and the corrected speed ($N/\sqrt{\theta}$).

2. A linear gradient of intake static pressure was assumed between the inner and the outer wall tapping readings. Static pressure values were computed on this basis for each of the four radii at which the total conditions were measured.

3. Four observed incremental mass flow rates were derived from total temperature, total and static pressures, and the geometrical area elements associated with

the probe locations. Each of these was then reduced to standard intake conditions in accordance with the appropriate local total temperature and pressure readings. Both observed and corrected incremental mass flows were summed and the two gross intake flow rates were printed out.

4. Each inter-row outer wall static pressure was first reduced to standard day entry conditions and then used to form a static:inlet total pressure ratio by dividing by the standard day intake total pressure of 29.92 "Hg.

5. Total temperature, total and static pressure, as measured at the yaw probe location, were reduced to standard entry conditions and are presented on the output sheets, together with the null-determined flow angle at outlet from the last row of stators. These values were appropriate to Position 3 (see Fig. 7).

6. Outlet total temperatures and pressures were averaged in the same manner as described for the inlet group in paragraph 1, and were corrected to standard day conditions.

7. Overall pressure ratio was obtained from the quotient of observed average total pressures at outlet and inlet. Adiabatic efficiency was then derived from the pressure ratio and the temperature rise.

8. Observed outlet mass flow was computed for three incremental areas corresponding to the radial locations of the total pressure probes on the efflux rakes in the same manner as for the inlet (see para. 3). Linear gradients were assumed again for the static pressure variation between the measured wall statics, and also for the temperature variation between adjacent total temperature probes on each five-point rake. The flow was assumed to be axial, based on outlet yaw probe values of less than 5° swirl. The observed incremental mass flows were summed and the total was reduced to standard entry conditions. An arbitrary 3% reduction was applied to the outlet mass flow to account for the boundary-layer displacement thickness at the measuring plane in the exit annulus. This value was suggested by Rolls Royce, based on their experience with this and similar compressors.

9. Leakage through the labyrinth seals in the rear of the test compressor was ducted rearward into the tunnel through two venturis. The standard calculation procedure, as described in Reference 1, was coded (including curve fitting of various coefficients and empirical constants) and was used to compute the observed leakage mass flow rate.

10. Observed leakage mass flow rate was added to the observed outlet flow rate to yield a total observed efflux mass flow. This was compared with the observed inlet mass flow and the difference recorded as a percentage of the inlet flow rate.

Major performance parameters are grouped on the lower right-hand corner of Output Sheet 1 for convenience (see App. B). The outlet mass flow is included in this grouping in preference to the inlet mass flow, as greater confidence is placed on the static pressures measured in the parallel efflux annulus. One may note the significant streamline curvature caused by the dynamometer fairing in the inlet airstream, which produces a static pressure gradient across the annulus that may vary significantly from the linear gradient assumed in computing the inlet flow rate.

5.2 Stage Characteristics

The aerodynamic characteristics of each stage were computed from experimental values of compressor inlet and outlet conditions, speed, and the interstage static pressures, together with the computed mass flow rate. In addition, annulus geometry, stage-by-stage work split, and mean stage outlet flow angle were required. The latter two parameters were based on design data as measured values were not available.

At the entry to Stage 3 (which is the first stage of V-2, 3 to 5) $\frac{\dot{m}\sqrt{T}}{AP}$ is formed using measured total temperature and total pressure at inlet. $\frac{p}{P}$ and $\frac{V_A}{\sqrt{T}}$ follow from compressible flow relationships, and these were used to compute the flow coefficient $\left(\phi \equiv \frac{V_A}{U_M}\right)$ for Stage 3.

At the interstage stations between Stages 3 and 4 and Stages 4 and 5, measured values of total pressure and total temperature were not available. Instead, outer wall static pressures were used and the total temperature was derived from an assumed work split. Use of tip static pressure measurements to represent the mean static pressure is justified as the design flow direction is axial at outlet from all stators. This was verified experimentally for the Stage 5 stators by the yaw probe data.

The same computational procedure as described for Stage 3 entry could now be employed at the Stage 3 to 4 and Stage 4 to 5 interstage planes. The work coefficient

$$\left(\psi \equiv \frac{\eta_{ST}\ K_p \Delta T_{ST}}{U_M^{\ 2}}\right)$$

was evaluated at these stations as well as the previously-defined flow coefficient. One may note that the value of ψ computed at, say, the Stage 3 to 4 interstage position refers to the preceding stage (Stage 3), whereas the value of ϕ computed at this same station refers to the subsequent stage (Stage 4).

At the outlet from Stage 5, measured total pressure and total temperature were again available and were used in the computational procedure for that last stage.

Major performance data, annulus geometry, and all assumed values (such as work split ratio) are presented with the stage characteristics on Output Sheet 2 (see App. B).

6.0 TEST RESULTS

6.1 Overall Compressor Performance

The computed parameters from the Data Reduction Routine were plotted as shown in Figures 8 to 24 inclusive. The comparable experimental data from Rolls Royce tests of "V-2, 3 to 5" are presented in Reference 2, and have been transcribed onto the appropriate plots in this report for convenience in comparing corresponding values.

As mentioned in Section 4.0, mechanical limitations prohibited operation of the NRC equipment at speeds above about 17,000 rpm. Consequently, few significant data were recorded at tip speeds of 1100 ft/sec or above. However, complete characteristic lines were obtained at tip speeds of 700, 800, 900, and 1000 ft/sec (i.e. up to about 80% of design speed).

6.1.1 Compressor Map

Figure 8 displays both pressure ratio (PR) and efficiency (η_{CT}) as functions of the Mass Flow Function ($\dot{m}\sqrt{T_{IN}}/P_{IN}$) based on the total outlet flow rate. Acceptably good agreement can be noted for all characteristics up to and including U_T = 1000 ft/sec. Temperature-based efficiencies, as determined on the NRC rig, appear somewhat higher than the Rolls Royce results, especially at very low speeds. Nevertheless, the curves appear smooth and are repeatable; minor discrepancies in temperature measurements may account for the differences. One can observe that at U_T = 700 ft/sec, $\Delta T_C \approx 30°C$ and therefore a 1°C uncertainty in temperature rise yields a 3% uncertainty in efficiency. In fact, NRC efficiency values differ from Rolls Royce values by, at most, 2%.

Very few useful data were obtained at NRC for the 1100-ft/sec characteristic. The points shown on Figure 8 are, in general, each from a different run, and therefore more scatter is to be expected than if all points were recorded during a single test. Even so, the available results indicate somewhat lower pressure ratios and efficiencies than were determined during the Rolls Royce tests.

The location of the surge line based on NRC test results was in extremely close agreement with the Rolls Royce data at all tip speeds achieved.

6.1.2 Inlet Axial Velocity Profiles

Figure 9 illustrates the geometric configurations and area variations of the several inlet airpaths associated with computational and experimental analyses of the V-2, (3 to 5) compressor. The RR Derby Rig intake was used for the experimental testing of the compressor at RR in Derby; the NRC rig intake is used for all phases of the Small Compressor Project at NRC, including Phase Zero as discussed in this report. The other two intake profiles shown on Figure 9 (RR Parallel Inlet and RR Computer) have been used in various computer analyses of V-2 (3 to 5) performed by RR for the Small Compressor Project and for their own purposes. Some of these analytic predictions made by RR are illustrated in Figure 7 of Reference 2. They suggest that the unusual entry configuration of the NRC apparatus should produce only minor changes in the incidence angles on the first rotating blade row. This Reference also presents, in Figure 8, the predicted V_A/U_T profile at an axial station 4.8 inches upstream of the Rotor 3 entry plane in the NRC rig intake. It is presumed that this profile is for U_T = 1100 ft/sec and a mass flow rate of approximately 20.9 lb_m/sec. NRC experimental data were obtained at a plane 7.23 inches upstream of the Stage 3 rotor entry plane (see Fig. 9 and A-2) where the annulus area was 157.1 sq in compared with 140.2 sq in for the RR calculation plane. For this reason, direct comparison of the flow coefficient (V_A/U_T) profiles is not justified. Moreover, the NRC data included only wall tapping static pressures and total temperatures and pressures at four radii (i.e. only wall-static pressures were measured). The straight line static pressure variation with radius adopted for the velocity and mass flow calculations in the NRC data reduction routine, taken in conjunction with the almost uniform total pressure profile, yielded a substantially linear velocity profile in all cases.

The predicted variations of V_A/U_T with tip speed and axial distance into the intake system were derived from RR computer analyses with the RR computer intake. These relationships are illustrated on Figures 10a and 10b respectively. Figure 10a also shows the predicted velocity profile for the NRC rig at the design tip speed of 1243 ft/sec, and illustrates the more uniform velocity profile to be expected from the NRC entry configuration.

Figure 10b shows the assumed linear velocity distribution at entry to the Stage 3 rotors, as derived from the NRC experimental data, in comparison with the predicted values replotted from Figure 10a. One can see that for this comparison the NRC experimental data had to be scaled by the area ratio between the RR calculation plane (140.2 sq in) and the NRC measurement plane (157.1 sq in). Despite the linear approximation, the NRC results are in satisfactory agreement with the RR predictions, particularly at the inner radius. At the outer radius, the measured velocity is greater than the predicted value by about 10%, which implies a change in tip incidence at the Stage 3 rotors of only about -2°.

6.1.3 Inter-Row and Interstage Static Pressures

As described in Section 3.3.3, inter-row static pressures were measured via tappings in the compressor annulus outer wall at the seven axial locations shown in Figure 7. Figure 11 shows a general selection of these data plotted on a common abscissa ($\dot{m}\sqrt{T_{IN}}/P_{IN}$) for the range of tip speeds covered in the abbreviated experimental program at NRC. Two primary observations are noticeable from this composite plot. First, the fifth-stage stators seem to produce negligible increase in static pressure, and second, the fourth-stage rotors appear to load up considerably as the tip speed increases.

The first of these two phenomena is more clearly shown on Figure 12, which depicts inter-row static pressure ratios for tip speeds of 700, 800, 900, 1000, and 1100 ft/sec at mass flow rates slightly below the surge value for each characteristic. Again, dashed lines have been used to bridge uncertainties or gaps in the available data. From this plot it can be clearly seen that the majority of the static pressure increase takes place in the rotating row of each stage. The stationary blade rows contribute significantly less and indeed, in the case of the fifth-stage stators, a slight pressure loss was recorded through the row at the lower tip speeds.

The relative contribution of each of the three stages is shown in Figure 13, again as a function of tip speed. It is evident from this plot that the third stage (Stage 51) is not producing as high a pressure ratio as would be expected from a compressor designed for approximately equal work in each stage. For comparison, the right-hand side of Figure 13 shows the stage total pressure ratios for a hypothetical compressor, of roughly the same overall pressure ratio as V-2, designed to produce equal temperature rise in each stage at equal stage efficiency. It can also be seen from this graph that the work done by Stages 3 and 4 respectively appears to be incorrectly proportioned, Stage 4 carrying considerably more than its equal share, especially at the higher tip speeds. One expects some variation of work-split with tip speed - usually the early stages tend to off-load and the later stages tend to load-up as speed increases. However, the proportions shown on Figure 13 did not follow this expected variation and the rapidly increasing load carried by Stage 4 suggests a slight mismatching of stage characteristics. Further discussion of possible causes of these and other stage phenomena appears in Section 6.2.

Figure 5 of Reference 2 (S-22869) shows the variation of tip static pressure at each inter-row station as a function of mass flow along a constant speed characteristic, viz 1000 ft/sec tip speed. Five points were selected from the NRC experimental results, at similar mass flows and pressure ratios, for comparison with these data from RR experiments. These comparisons, shown in Figures 14a to 14e, demonstrate good agreement between the two data sources for the majority of inter-row locations. However, the NRC data indicate a slight static pressure drop across the Stage 5 stators, whereas the RR data indicate a static pressure rise about equivalent to that across the other stator rows. Moreover, the limited amount of data recorded at NRC from the traversing yaw probe confirmed the flow direction at exit from the Stage 5 stators to be within five degrees of axial at all radial positions. Consequently, no satisfactory explanation has been found for this anomalous decrease in static pressure.

6.1.4 Outlet Radial Total Pressure and Total Temperature Profiles

As shown in Figures 6 and A-2, the outlet pressure and temperature instrumentation was located as follows:

Total Pressure Rake (4 off, 3 radial locations each)
4.57 inches downstream of fifth stator trailing edges.

Static Pressure Wall Tappings (4 off in each inner and outer wall)
5.85 inches downstream of fifth stator trailing edges.

Total Temperature Rake (4 off, 5 radial locations each)
6.10 inches downstream of fifth stator trailing edges.

All sensing ports were located circumferentially so as to avoid any wakes that might have been shed from the eight uncambered dummy outlet guide vanes whose trailing edges were 3.91 inches downstream of the trailing edges of the Stage 5 stators.

Figures 15, 16, and 17 compare the radial variations of total pressure and total temperature in the compressor outlet annulus, at tip speeds of 1000 ft/sec and 1100 ft/sec, with RR experimental data from Figure 2 (S-24397) and Figure 3 (S-22867) of Reference 2. Test points were selected from the NRC data at positions on the constant speed characteristics that corresponded reasonably closely in overall total pressure ratio and mass flow rate to the RR data points.

The RR total pressure data have been replotted, together with the NRC results, on Figure 15. The small horizontal arrows on each curve indicate the mean outlet total pressures for both data sources. The Figure illustrates the close agreement of results from the two experimental programs, both as to shape of the curves and magnitude of variations with radius, despite the fact that the RR data were taken 2.57 inches upstream of the NRC instrumentation station, closer to the trailing edges of the Stage 5 stators.

In a similar manner to the pressure data, the outlet total temperature profiles and mean values are shown on Figures 16 (U_T = 1000 ft/sec) and 17 (U_T = 1100 ft/sec) in comparison with RR data from Reference 2, Figures 3 (S-22867) and 4 (S-22868).

From Figure 16 it is seen that at U_T = 1000 ft/sec the general trend of increasing temperature ratio from inner wall to outer wall is confirmed, although the NRC data indicate a greater spread across the annulus, viz ~10°C c.f. ~6°C. For the higher mass flow points, data from the two sources agree very well at the inner wall but the NRC results show considerably higher temperatures at the outer wall.

Nevertheless, the mean values computed from pressure ratio and efficiency values agree reasonably well, considering the amplified ordinate scale and the accuracy and reliability of the outlet temperature values.

For points closer to the surge line, the agreement appears to shift towards the outer wall with the NRC inner wall temperatures (and the mean values) being some 4°C lower than the RR values. This is undoubtedly caused by the somewhat lower pressure ratios near the surge point observed during the NRC tests. One may note from the insert that NRC Run No. 30.1521 lies at the pressure ratio of RR data point #4, but at a mass flow closer to that of RR data point #5.

As both sets of data were recorded at approximately the same axial position, one would expect the NRC results to show the same magnitudes and variation as those from RR experiments. However, the NRC curves are considerably smoother than the comparable RR curves, and one might consider that the thermocouple at 6.75 inches radius in the RR rig was reading erroneously high, thus giving rise to the inflection points in their curves.

At 1100 ft/sec tip speed (see Fig. 17) the NRC data again show higher outlet temperatures and wider variations with radius, although the RR data do not exhibit the inflection points noted in the results at U_T = 1000 ft/sec. Mean values marked by horizontal arrows on the NRC curves appear to lie at the expected values and are remarkably consistent in radial position (ranging only from 6.90 to 6.93 inches radius) for all flow rates plotted on the 1100 ft/sec characteristic.

The average outlet temperatures calculated from RR pressure ratio and efficiency data are strongly influenced by minor changes in the air specific heat value chosen. For example, an increase from 0.240 to 0.241 changes the value of $\frac{\Delta T_c}{T_{IN}}$ from 0.3445 to 0.3535 and the corresponding radius of the average value from 6.88 to 7.19 inches.

This sensitivity to specific heat, together with the lack of close agreement between the NRC and RR test points, prohibits any detailed comparisons between the data sets. As can be noted from the insert on Figure 17, the NRC pressure ratios were substantially lower at most mass flow rates than were the RR data points along this 1100 ft/sec speed line. Moreover, as outlined in Section 6.1, the NRC data, being comprised of single data point recordings taken during a number of preliminary runs, do not have the internal consistency of the other speed lines.

6.2 Stage Characteristics

The three parameters that define the operating characteristics of an axial compressor stage are listed below:

Flow coefficient $$\phi \equiv \frac{V_A}{U_M}$$

Work coefficient $$\psi \equiv g_o \, J \, Cp \, \eta_{ST} \, \Delta T_{ST} / U_M^2$$

Stage efficiency η_{ST} (adiabatic) $$\equiv \frac{\Delta h)_{isentropic}}{\Delta h)_{actual}} \approx \frac{\Delta T)_{isentropic}}{\Delta T)_{actual}}$$

These nondimensional groupings were calculated for each test point using the procedure detailed in Section 5.2. One should recall that the calculation of the stage characteristics was based on outer wall static pressure measurements (as an approximation of mean static pressures between the blade rows) and the previously computed outlet mass flow. The stage work split (i.e. the fraction of the overall total temperature rise that is produced by each stage) was the only independent variable required in addition to the compressor annulus geometry and the quantities computed during the overall performance calculations. Ideally, the total temperature would have been measured at the outlet from each stage. These measurements were not provided and therefore the work split fractions for Stage 3, Stage 4, and Stage 5 had to be assigned for the calculation routine. This somewhat arbitrary procedure is acceptable inasmuch as stage characteristics based on such sparse instrumentation form, at best, bases for qualitative rather than quantitative assessments, especially at part speeds.

Initially, the three stages were assumed to produce equal fractions of the overall temperature rise at all tip speeds. Results based on this division of temperature rise are shown on Figures 18 to 20 inclusive, for tip speeds of 700, 800, and 1000 ft/sec. Part (a) of each of these Figures shows the variations of ψ with ϕ for all three stages, and part (b) depicts the η_{ST} vs ϕ relationships.

In general, there is considerable scatter in both ψ and η_{ST} data as determined from the NRC tests. Some irregularities were expected where raw data were gathered as a series of single points recorded during different runs; however, during the latter part of the experimental program entire constant-speed characteristic lines were systematically defined during a single run and yet the discrepancies are still large. Agreement with the limited amount of analytic and experimental results provided by RR is not good in terms of absolute values, although the majority of the NRC characteristic curves are smooth and have the expected shapes and slopes.

These observations suggested that a constant (with tip speed) equal work split was not, in fact, a good approximation to the real process, especially at lower tip speeds, where it can be noted that Stage 3 efficiencies are absurdly high and Stage 5 efficiencies are unrealistically low.

As all three stages are very similar in design, it seemed reasonable to expect that they should exhibit relatively similar characteristic curves. Accordingly, for each tip speed, data from all stages were plotted on common η_{ST} vs ϕ and ψ vs ϕ co-ordinates. Work split fractions were then adjusted by trial and error to achieve a smoother variation of stage efficiency for all stages over the entire flow coefficient range. Examples of the effect of different work split fractions are shown in Figures 18c and d, 19c, and 20c for stage efficiency and work coefficient respectively. It can be clearly seen that at 700 ft/sec tip speed, work split fractions of 0.482, 0.311, and 0.207 for Stages 3, 4, and 5 respectively, yield much smoother and more realistic variations in stage efficiency, and that the work coefficients are relatively unchanged. This procedure was repeated (Fig. 19c and 20c) for the 800 ft/sec and 1000 ft/sec constant speed characteristics and the resultant variation of work split and tip speed was determined to be as shown in Figure 21.

Based on this artificially determined variation of fractional temperature rise, the characteristics for each stage for all available tip speeds were combined as shown on Figures 22a and b to 24a and b.

7.0 CONCLUSIONS

1. Overall performance parameters from the NRC tests agree satisfactorily with results from an RR experimental evaluation of another compressor of the same aerodynamic design, over the limited range achieved in the present program. At a tip speed of 1000 ft/sec (80%) - the highest speed at which reliable data were obtained during the NRC experiments - the three-stage compressor achieved a peak pressure ratio of 2.21 and a peak efficiency of 84%, compared with 2.17 and 85% respectively from the RR data. Other, lower, speed lines showed equally good agreement in pressure ratio and flow range, although the NRC-measured efficiencies were up to 1.5% higher than the RR values.

2. The experimentally determined surge line was essentially identical in both the NRC and the RR tests.

3. The individual stage characteristics derived from the NRC test data showed unacceptably high scatter and very poor agreement with the corresponding RR test values. The unsatisfactory nature of the NRC test data was, at least in part, due to the sparse interstage instrumentation provided in the Phase Zero test unit. Specifically, no interstage temperatures were measured, and stage characteristics had to be derived from assumed proportions of the overall compressor temperature rise. Agreement with the RR characteristics improved somewhat with manipulation of these work split proportions away from the initially assumed equal values. The fact that the overall compressor performance agreed well with the RR results suggests that the Phase Zero test compressor was operating as expected and that deviations in the stage characteristics must be attributable to measurement or analysis techniques.

8.0 REFERENCES

1. Flow Measurement.
   British Standard Code B.S. 1042:1943 (incorporating amendments to October 1951).

2. Hopwood, D. J.
   Rolls-Royce Limited, Compressor Department Report RCR 90215, 2 June 1969.

3. Chappell, M. S.
   Sharp, C. R.
   Data Reduction Routine for Performance Tests on a Three-Stage Axial Compressor.
   NRC, DME Report to be published.

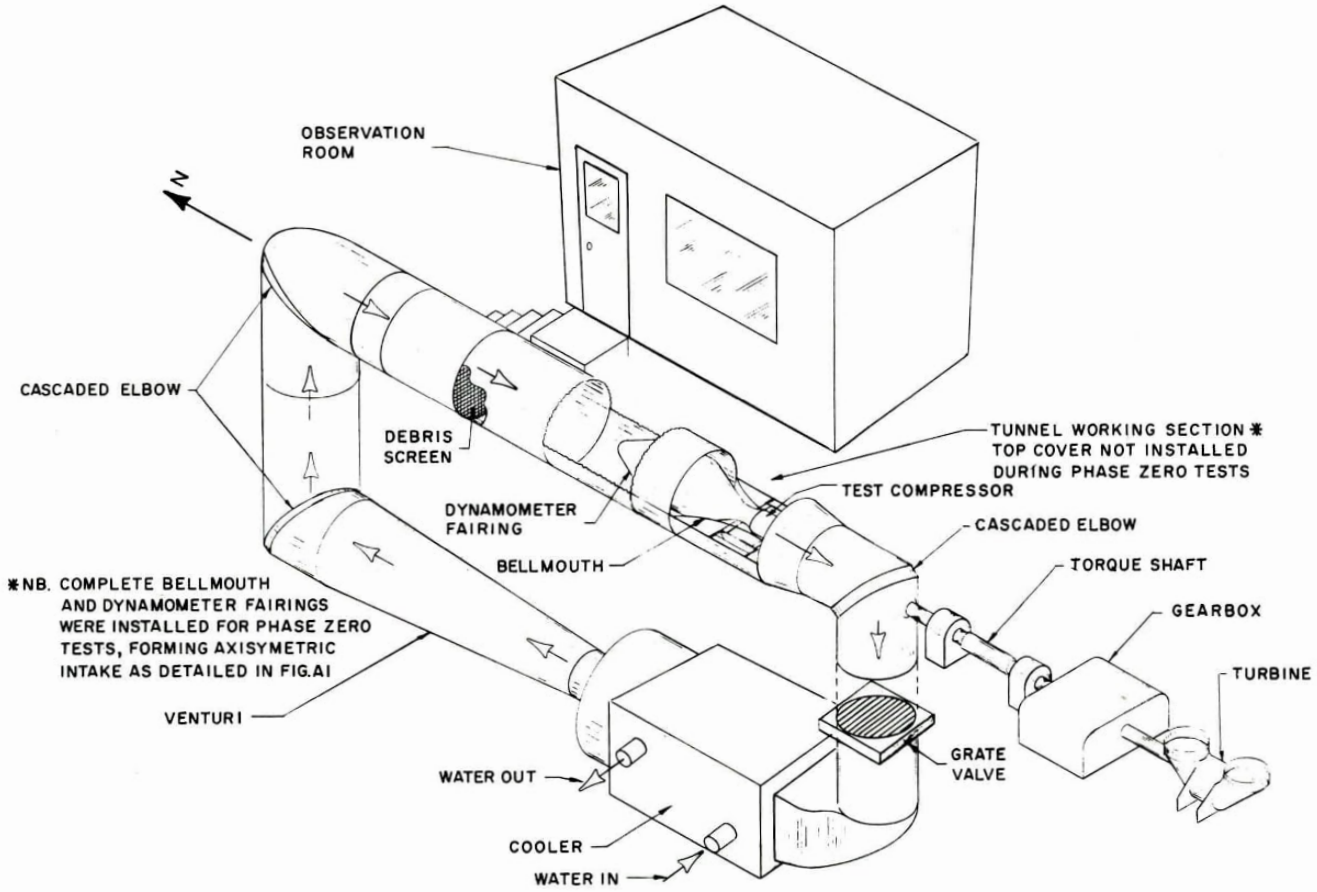

FIG. 2 : VARIABLE DENSITY COMPRESSOR TEST FACILITY : GENERAL LAYOUT

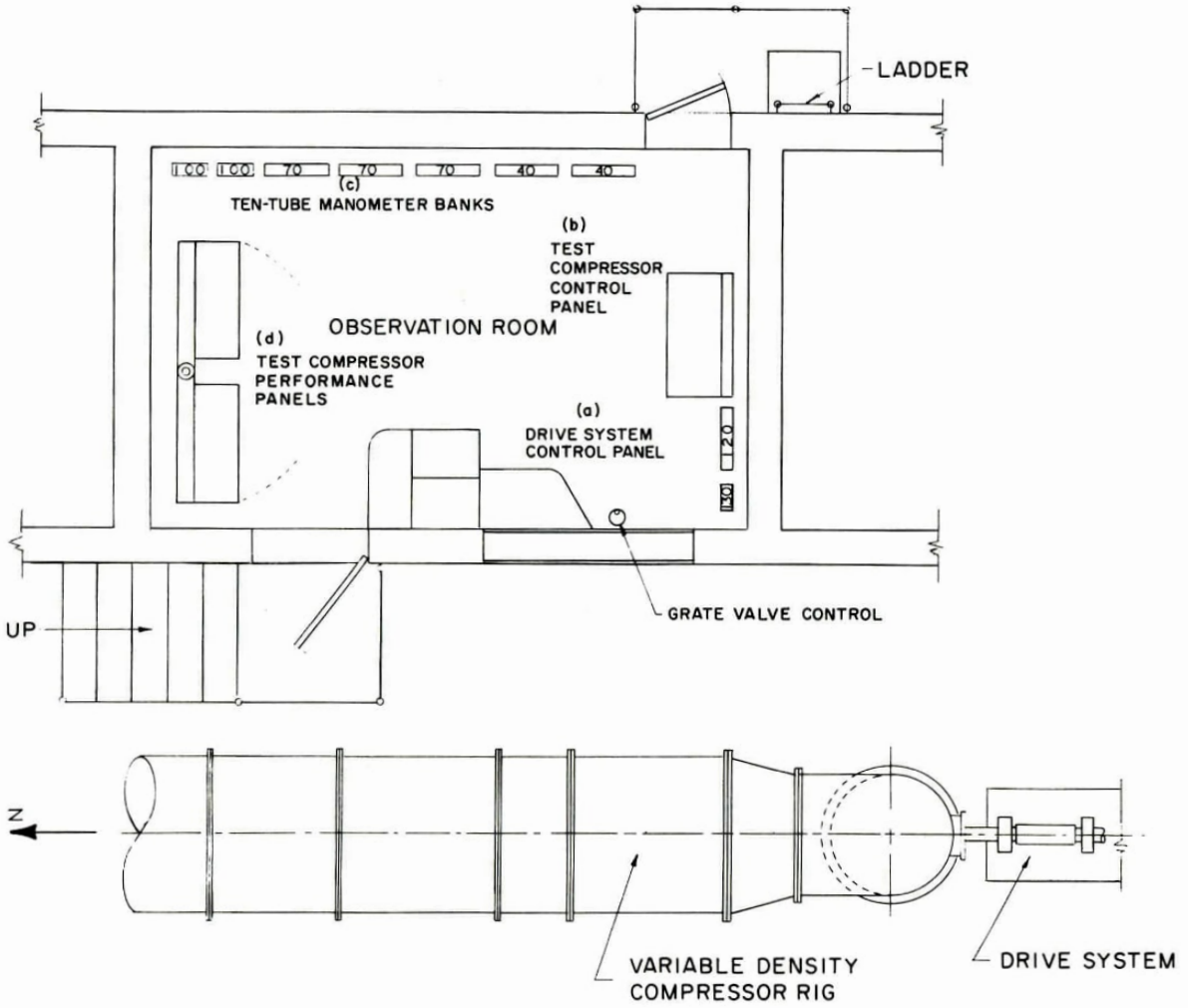

FIG. 3 : OBSERVATION ROOM LAYOUT — VARIABLE DENSITY COMPRESSOR TEST RIG

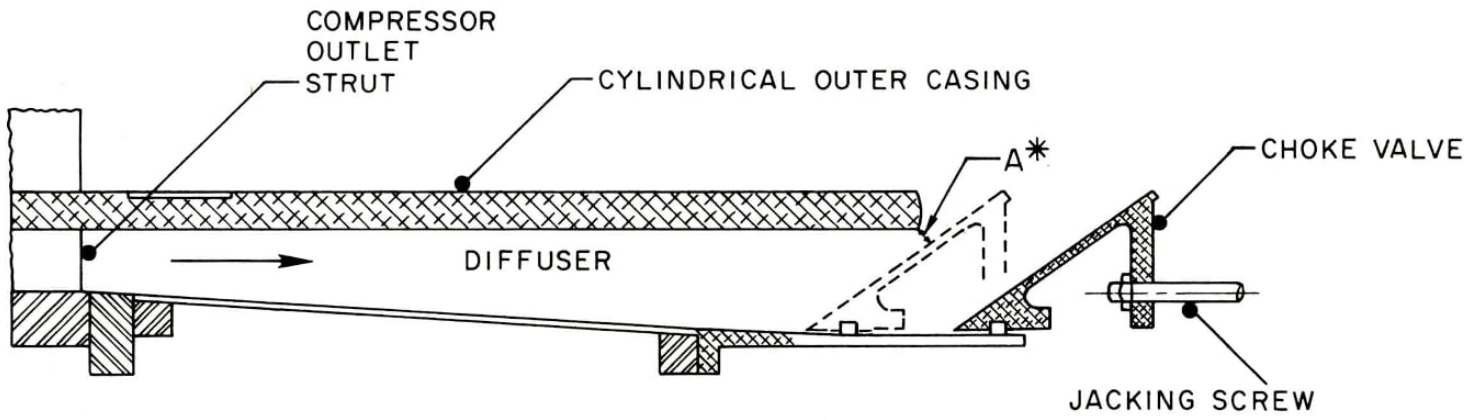

FIG. 4 : TEST COMPRESSOR OUTLET THROTTLE VALVE

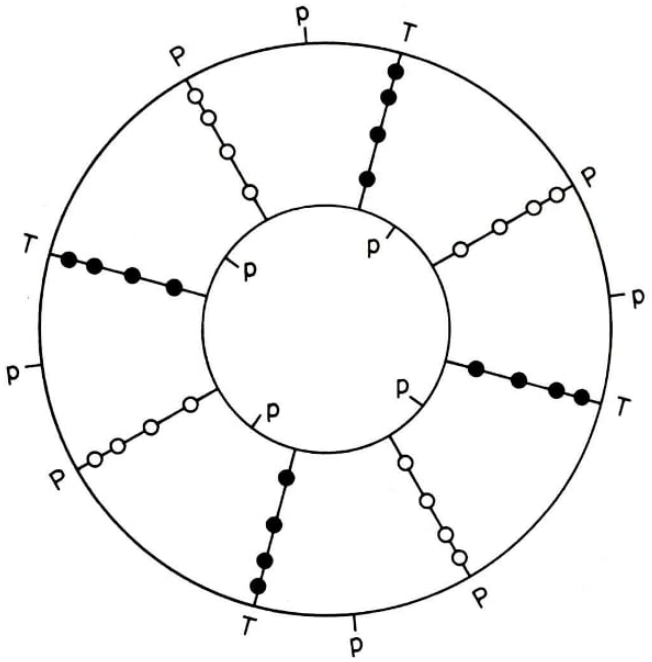

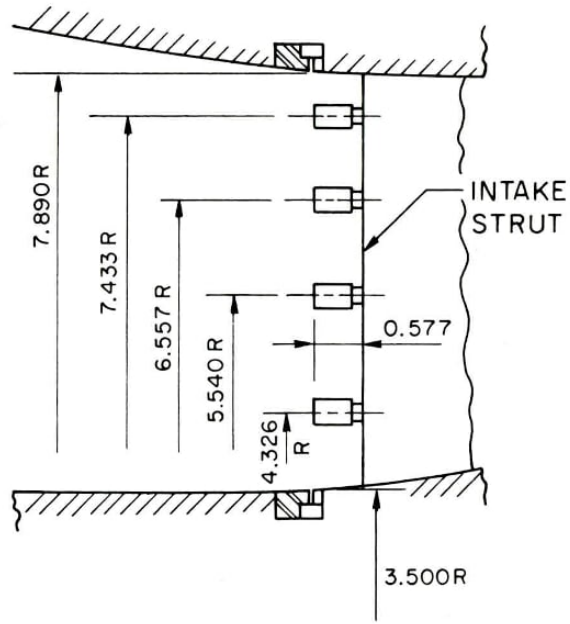

FIG.5 : INLET INSTRUMENTATION

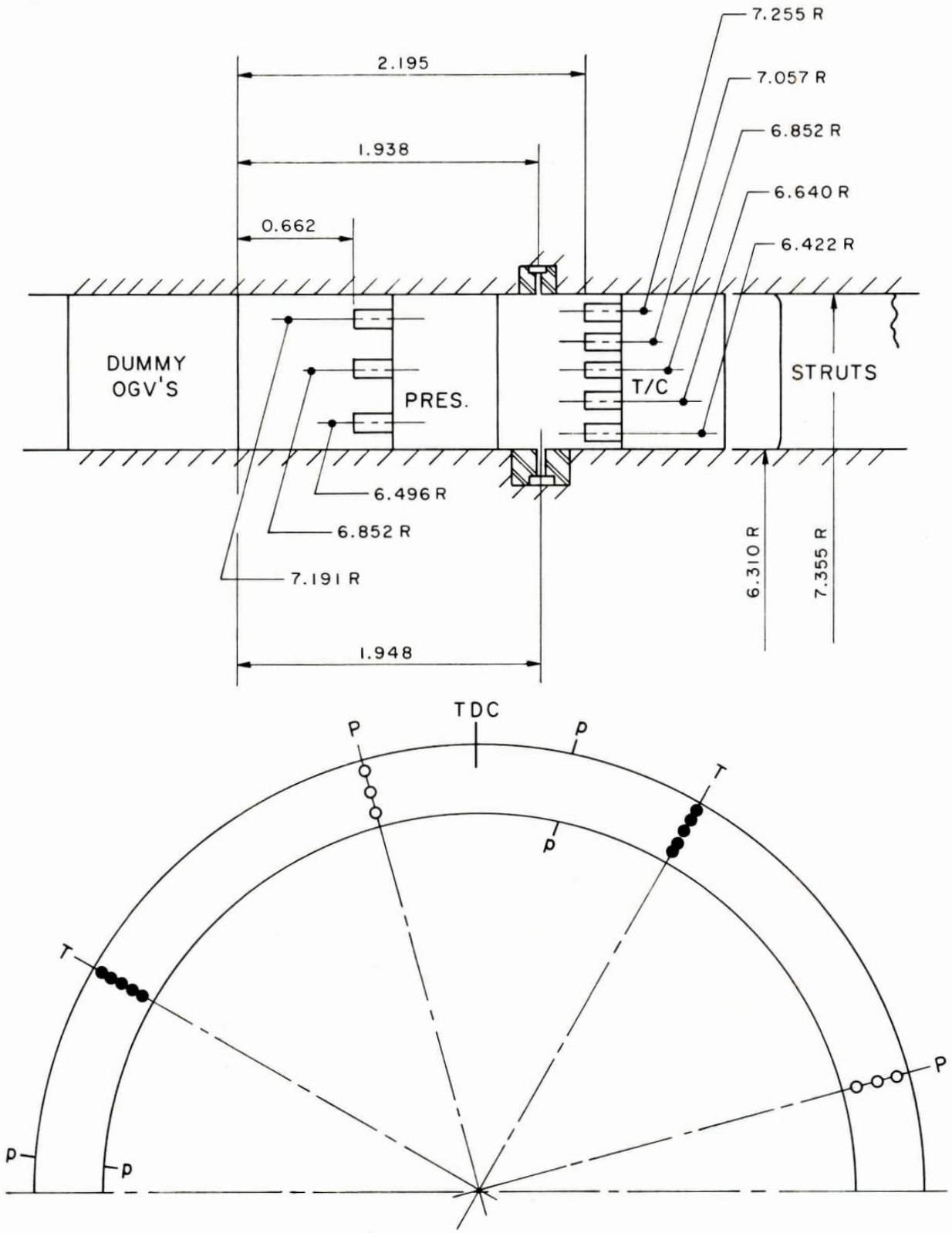

FIG.6 : OUTLET INSTRUMENTATION

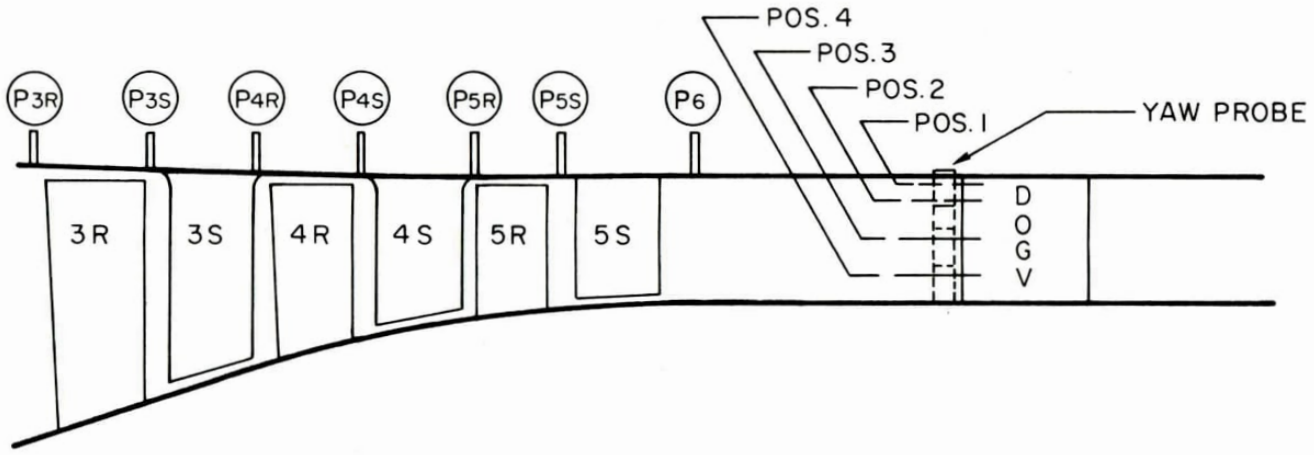

FIG. 7 : INTER-ROW INSTRUMENTATION AND OUTLET YAW PROBE

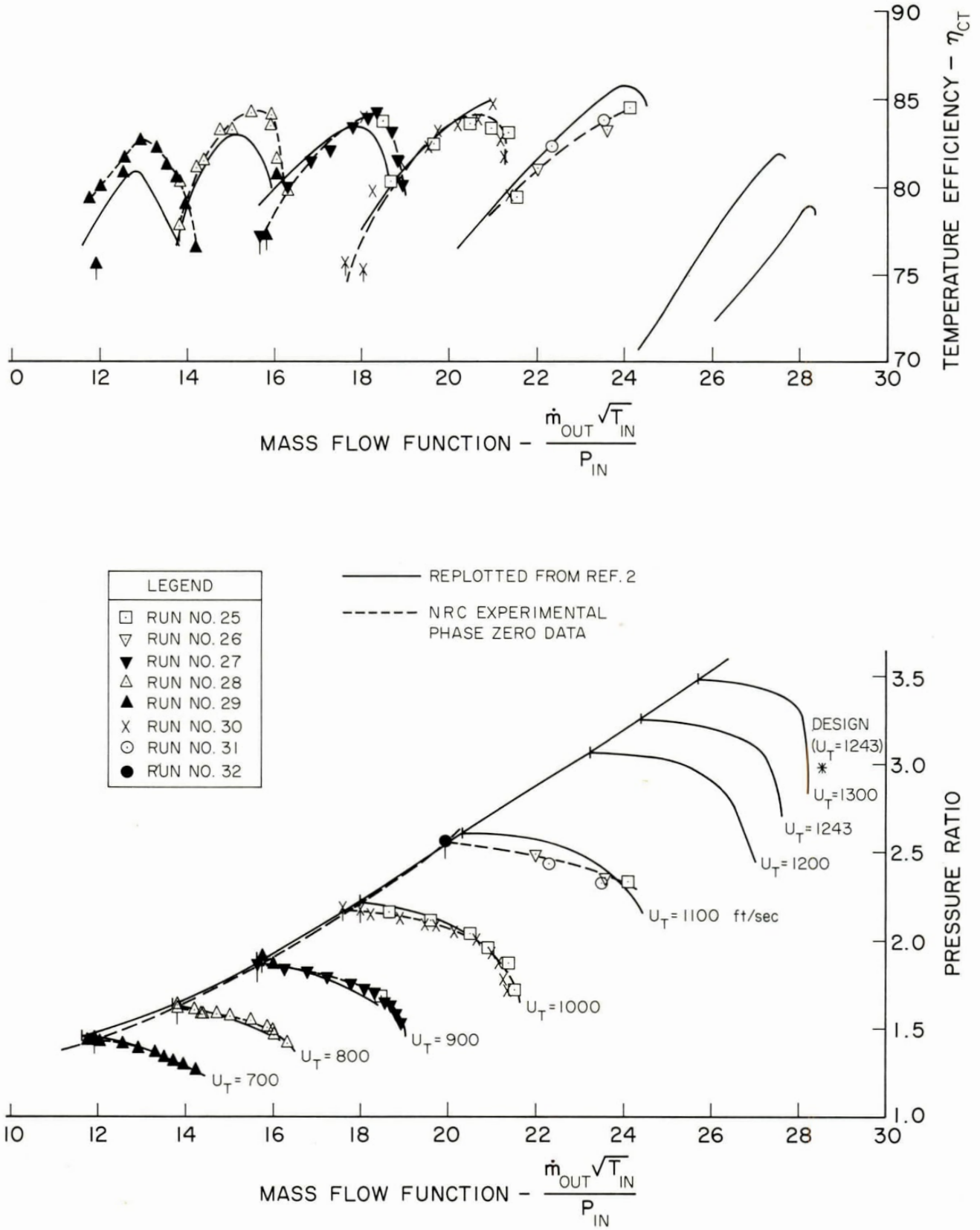

FIG. 8 : COMPRESSOR PERFORMANCE MAP

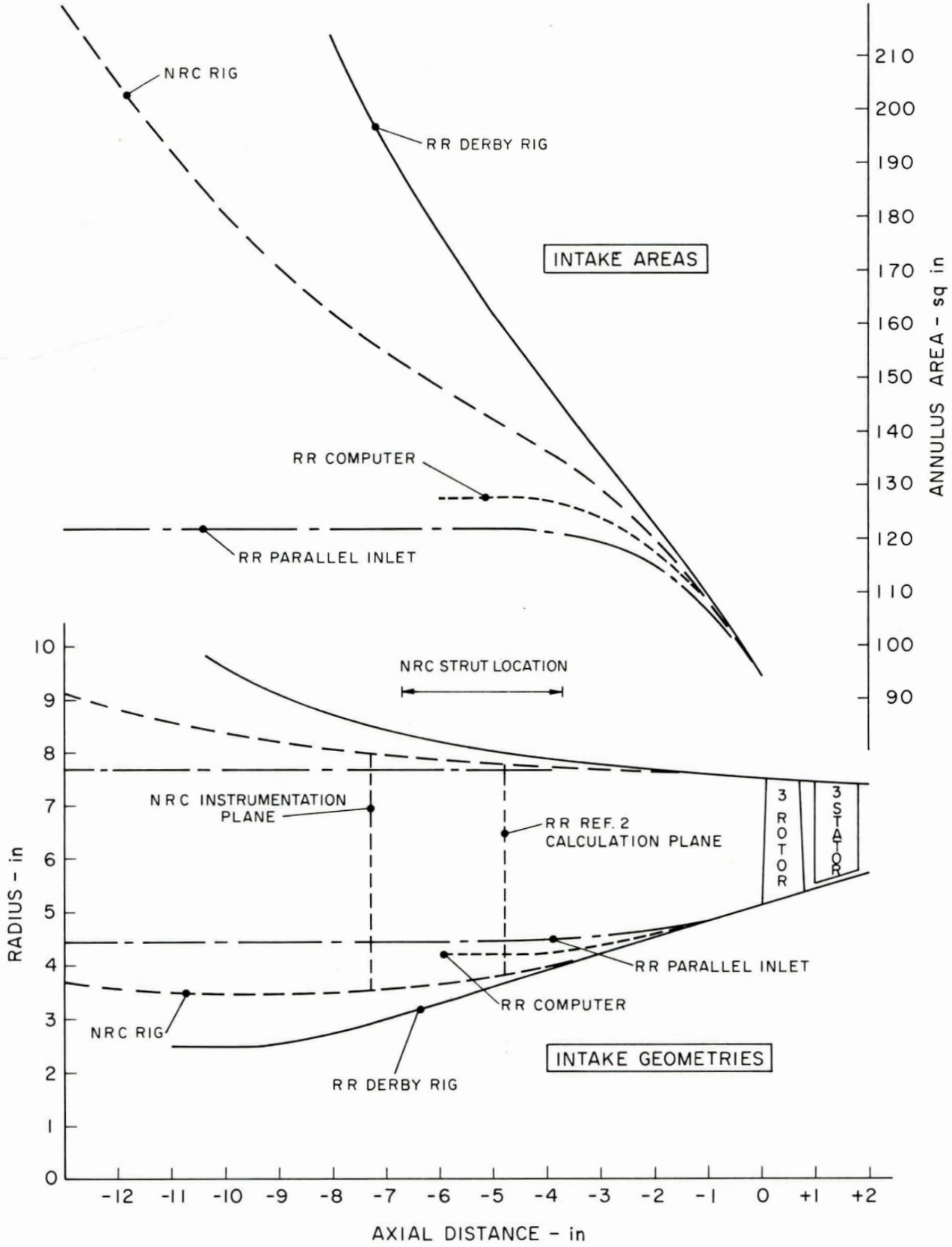

FIG. 9 : INLET DUCT CONFIGURATIONS

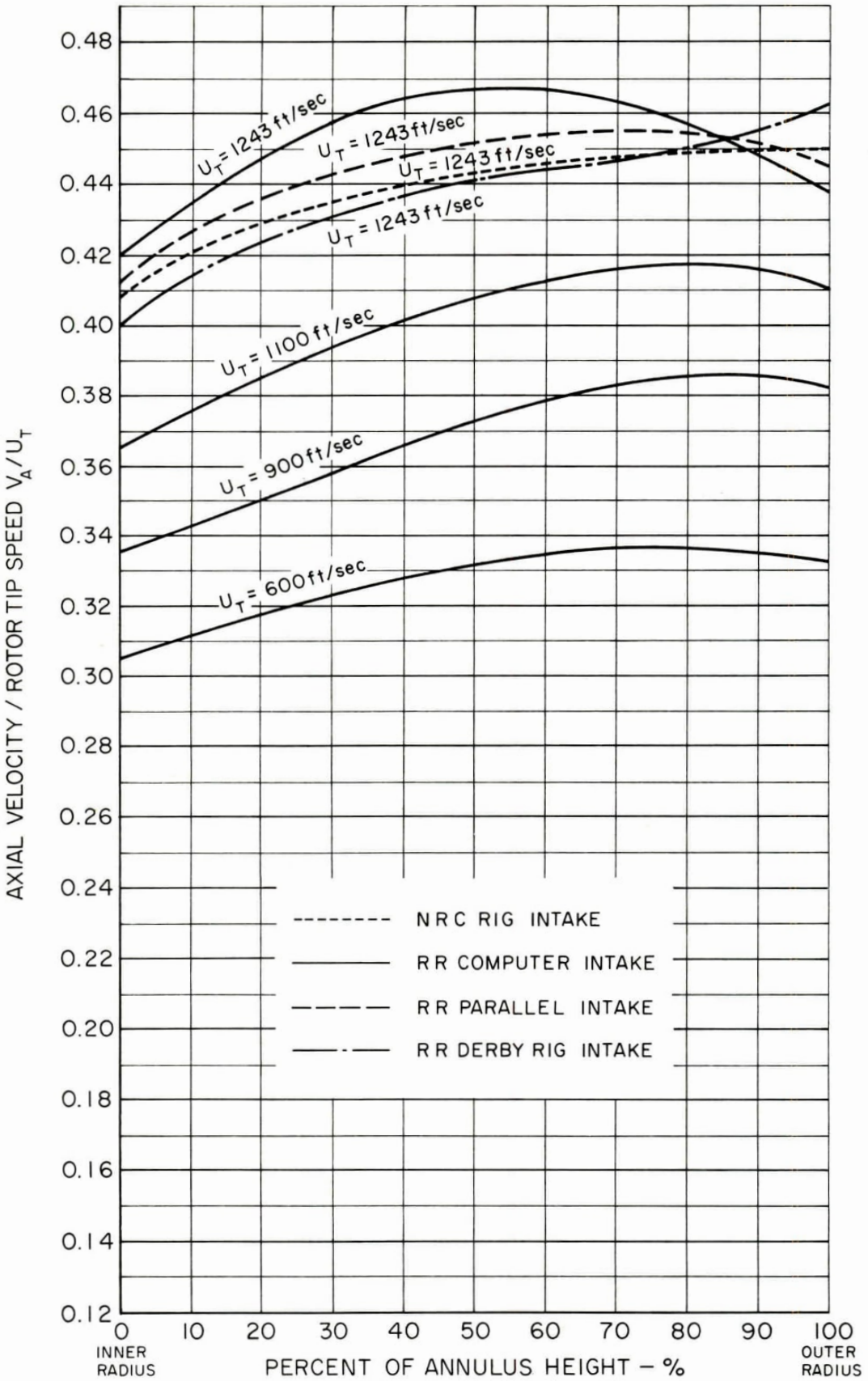

FIG. 10a : PREDICTED INTAKE VELOCITY PROFILES AT 3 ROTOR ENTRY
EFFECTS OF INTAKE GEOMETRY AND COMPRESSOR SPEED

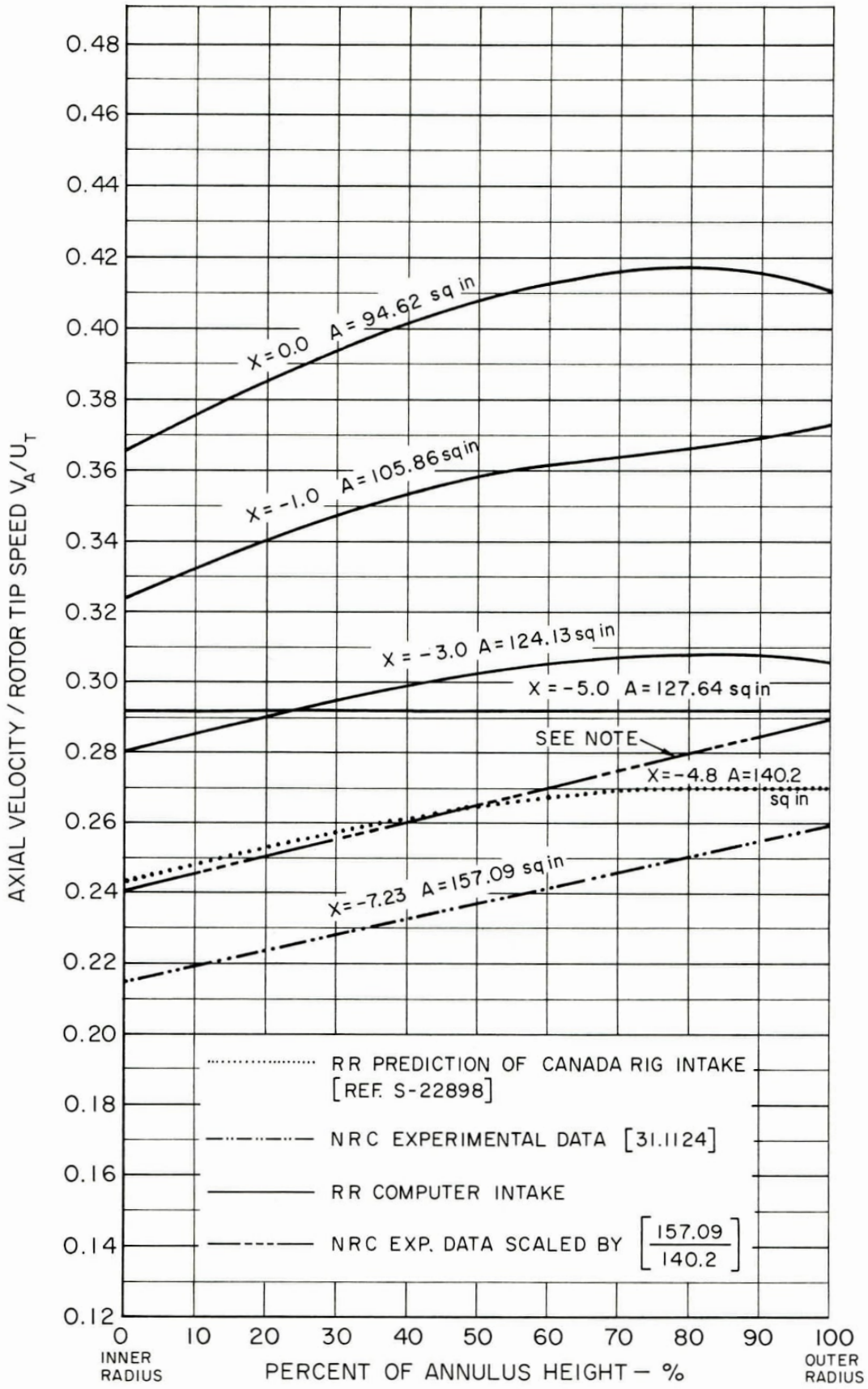

FIG. 10b : UPSTREAM INTAKE VELOCITY PROFILES AT U_T = 1100 ft/sec
EFFECT OF AXIAL LOCATION AND COMPARISON WITH PHASE ZERO EXPERIMENTAL RESULTS

FIG. 11 : INTER-ROW STATIC PRESSURE RATIOS vs MASS FLOW

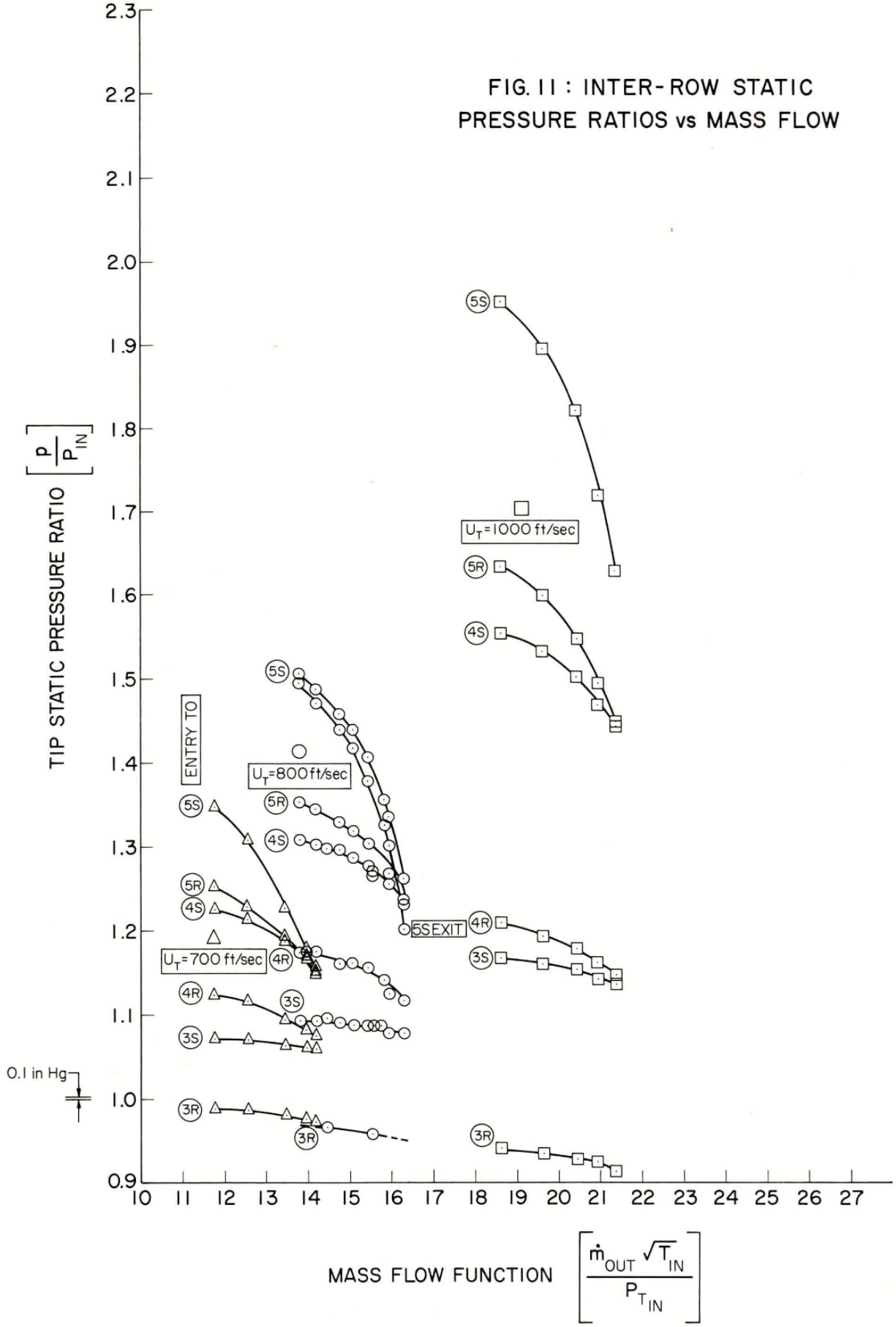

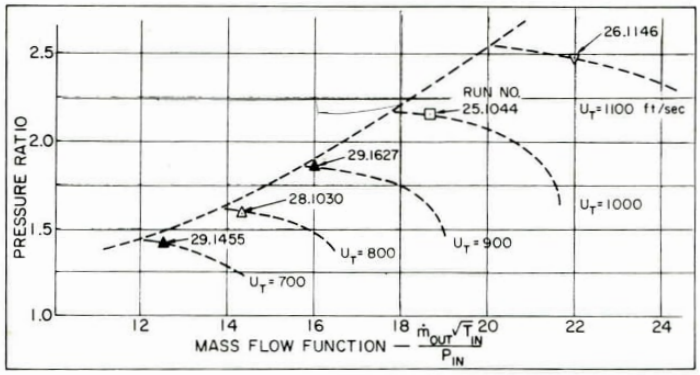

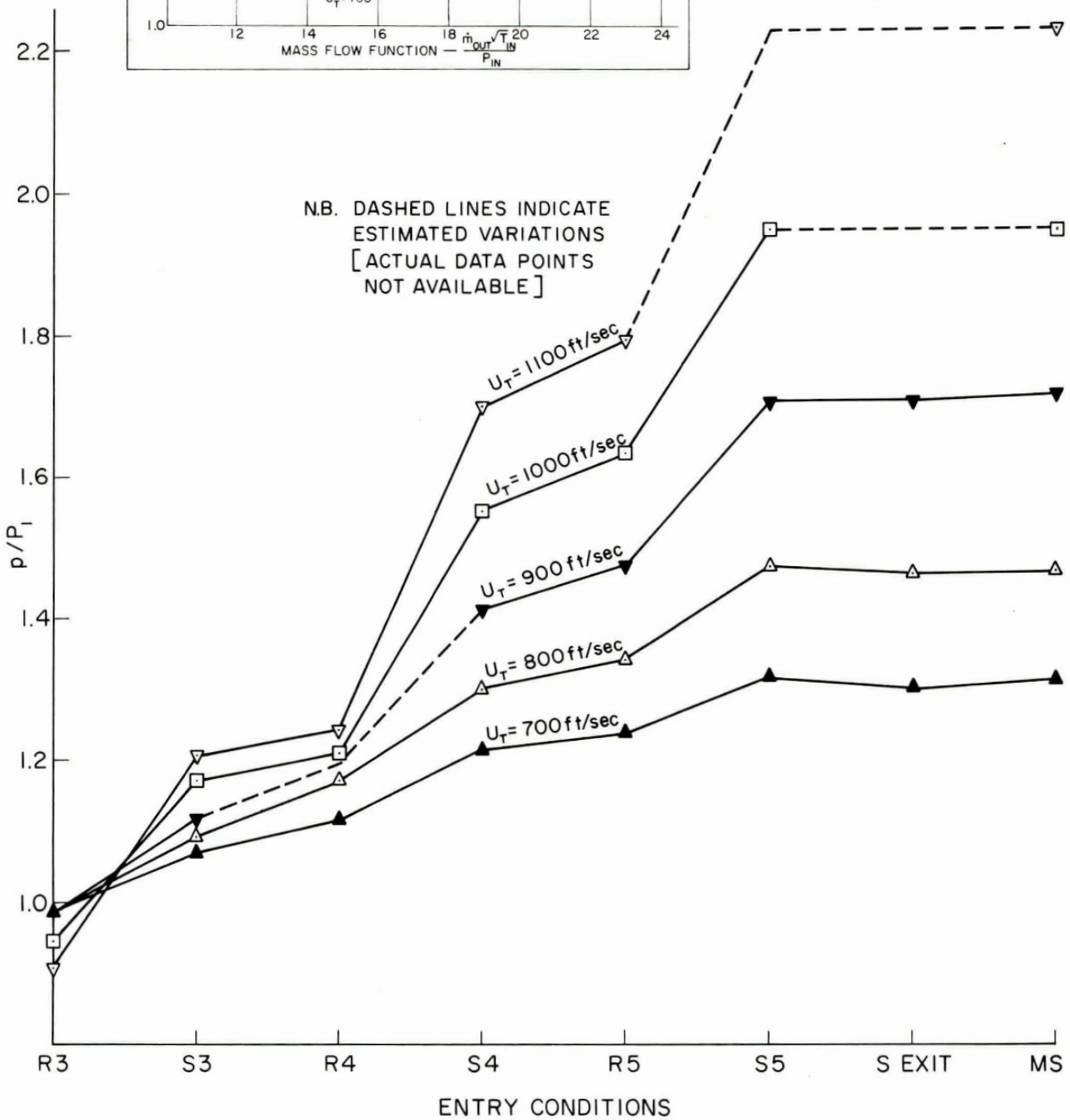

FIG.12 : INTER-ROW STATIC PRESSURE RATIOS vs AXIAL LOCATION

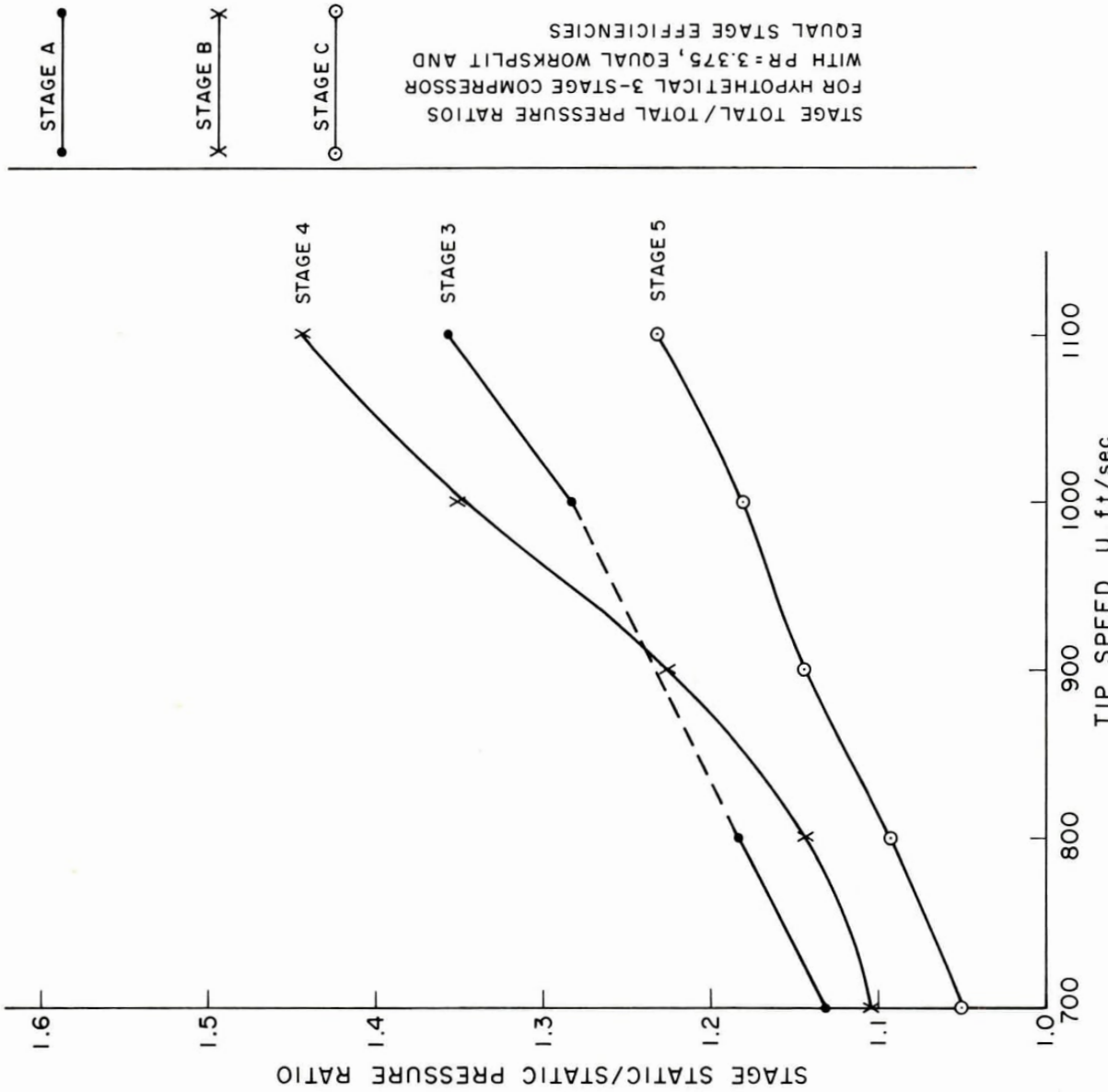

FIG.13 : STAGE STATIC PRESSURE RATIOS

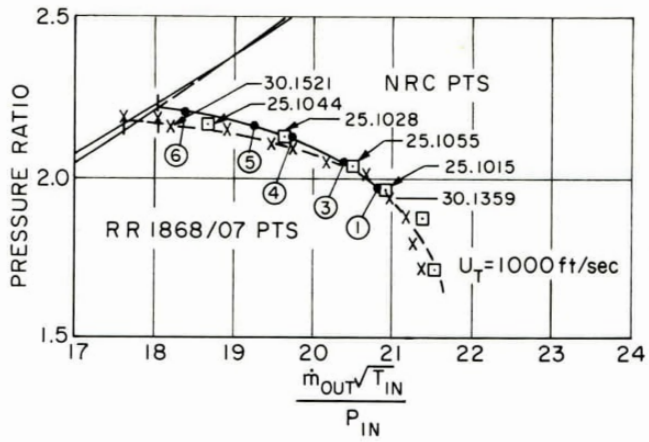

SUB-FIGURES (a) TO (e) REPRESENT PROGRESSIVELY DECREASING MASS FLOWS ALONG THE 1000 ft/sec CHARACTERISTIC APPROXIMATING POINTS ①,③,④,⑤, & ⑥ ON FIGURES 1 AND 5 OF REF. 2

[RR S22865 AND RR S22869]

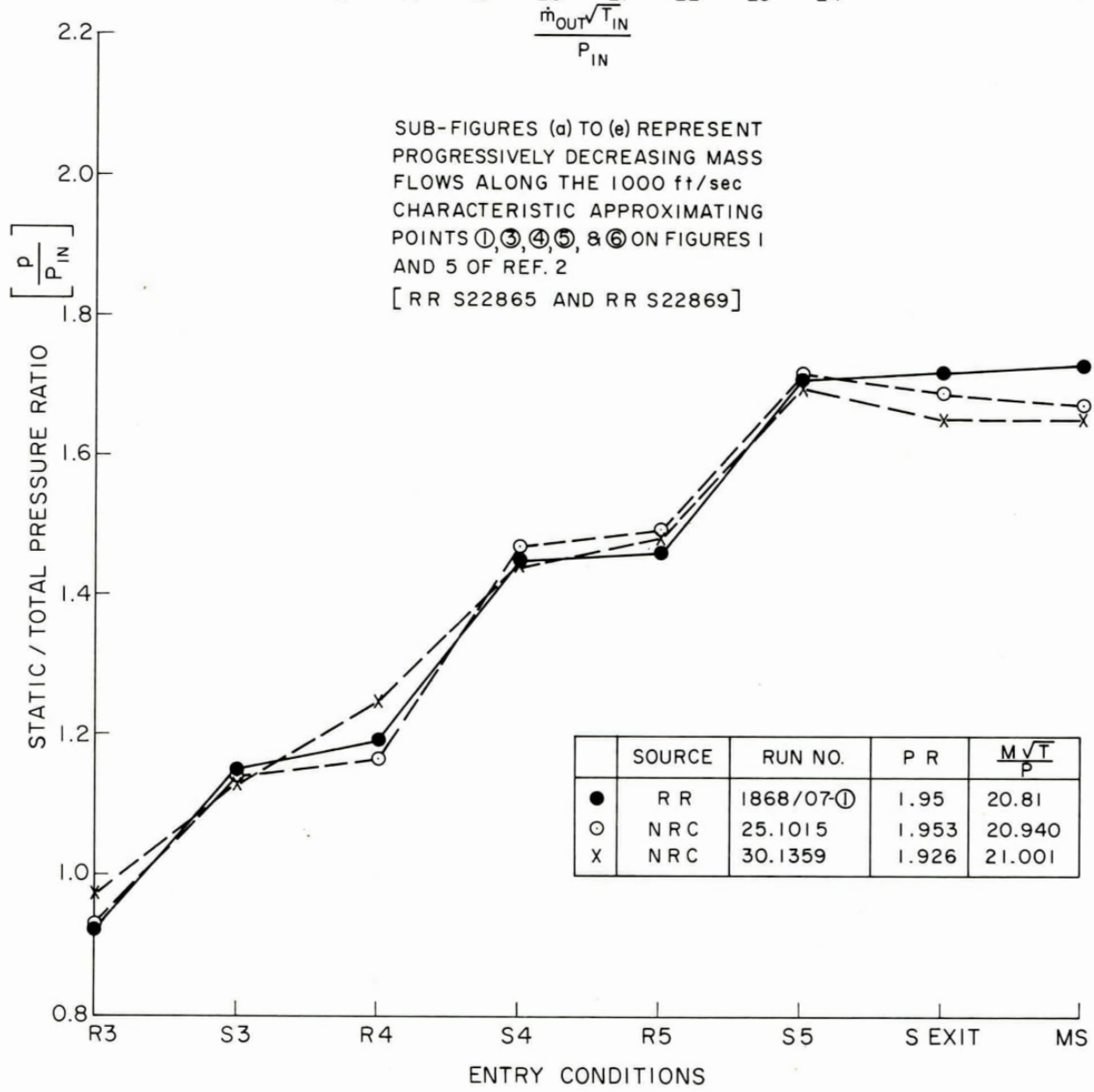

	SOURCE	RUN NO.	P R	$\frac{M\sqrt{T}}{P}$
●	R R	1868/07-①	1.95	20.81
⊙	N R C	25.1015	1.953	20.940
X	N R C	30.1359	1.926	21.001

FIG. 14a : INTER-ROW STATIC PRESSURE RATIOS

U_T = 1000 ft/sec

(b)

	SOURCE	RUN NO.	P R	$\frac{M\sqrt{T}}{P}$
●	RR	1868/07-③	2.05	20.43
⊙	NRC	25.1055	2.039	20.435

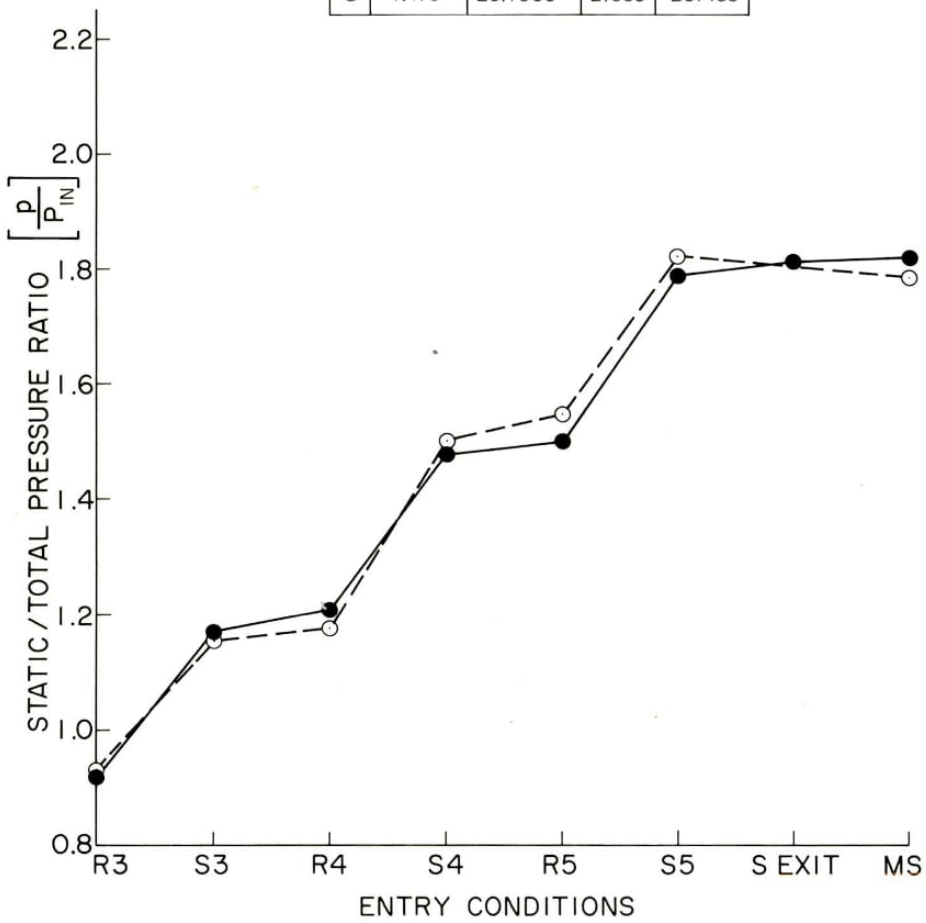

(c)

	SOURCE	RUN NO.	P R	$\frac{M\sqrt{T}}{P}$
●	RR	1868/07-④	2.11	19.72
⊙	NRC	25.1028	2.109	19.61

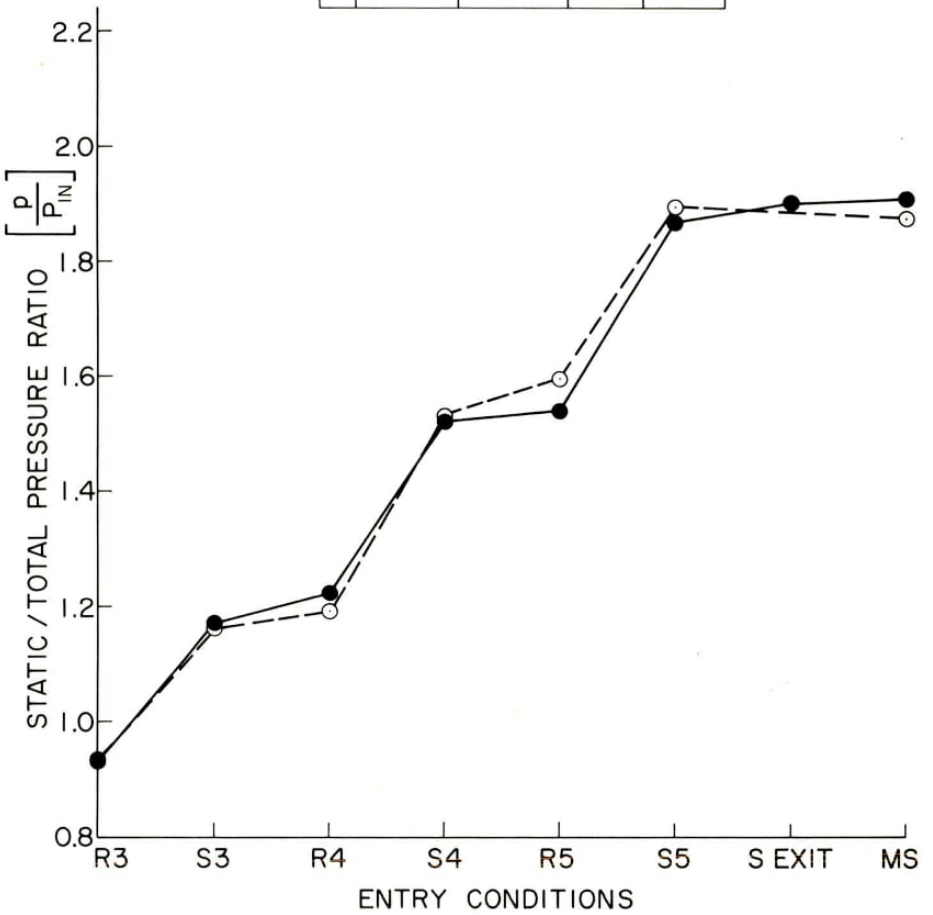

FIG. 14b,c : INTER-ROW STATIC PRESSURE RATIOS

U_T = 1000 ft/sec

(d)

	SOURCE	RUN NO.	PR	$\frac{M\sqrt{T}}{P}$
●	R R	1868/07-⑤	2.15	19.22
⊙	N R C	25.1044	2.155	18.621

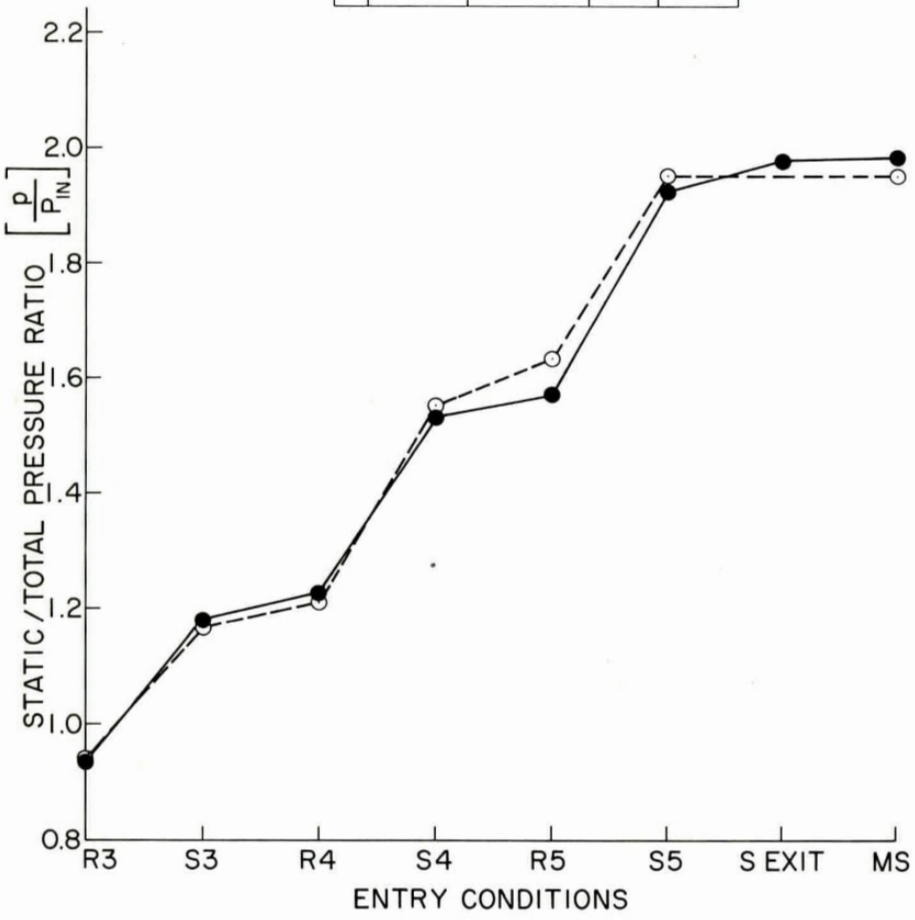

(e)

	SOURCE	RUN NO.	PR	$\frac{M\sqrt{T}}{P}$
●	R R	1868/07-⑥	2.20	18.40
⊙	N R C	30.1521	2.149	18.225
△	N R C	25.1044	2.155	18.621

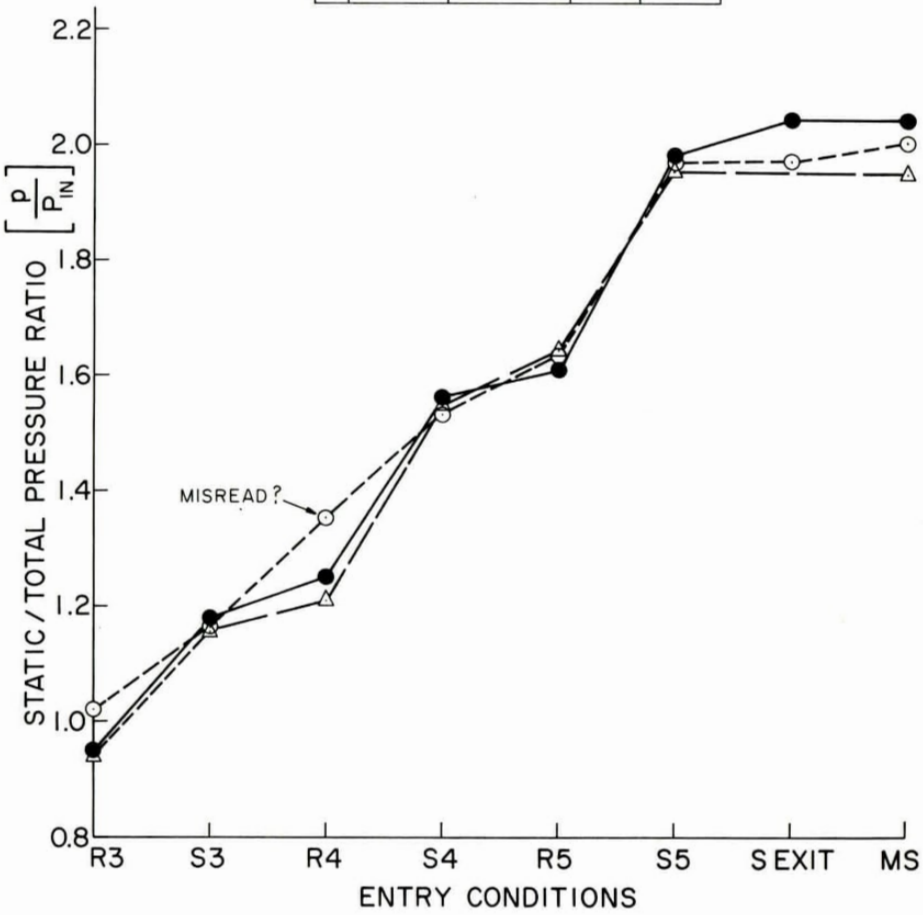

FIG. 14 d,e : INTER-ROW STATIC PRESSURE RATIOS

U_T = 1000 ft/sec

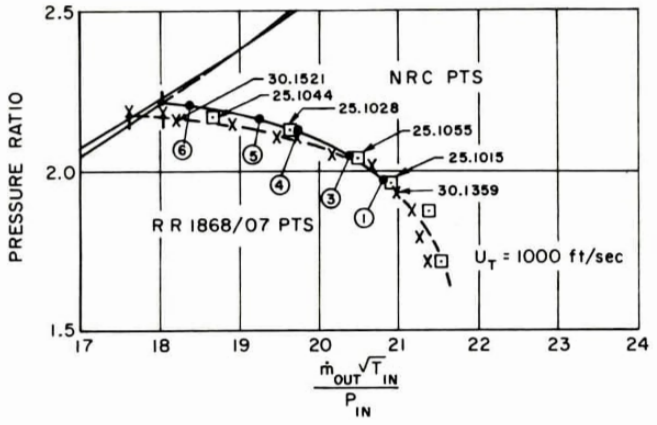

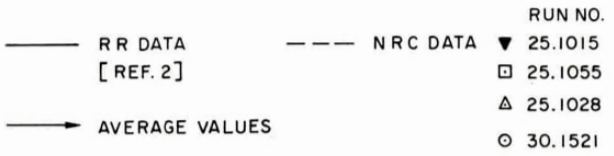

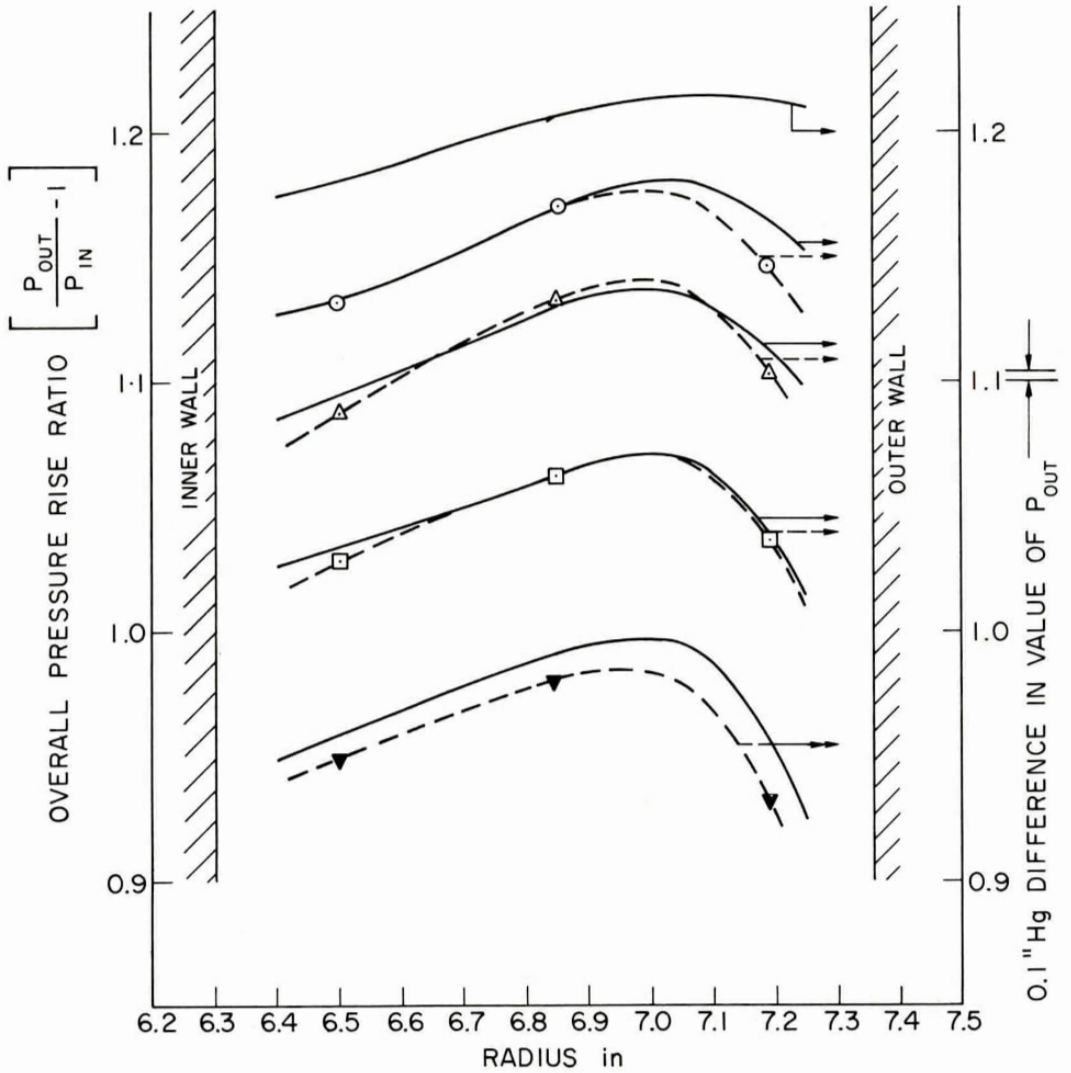

FIG.15 : OUTLET TOTAL PRESSURE PROFILES — U_T = 1000 ft/sec

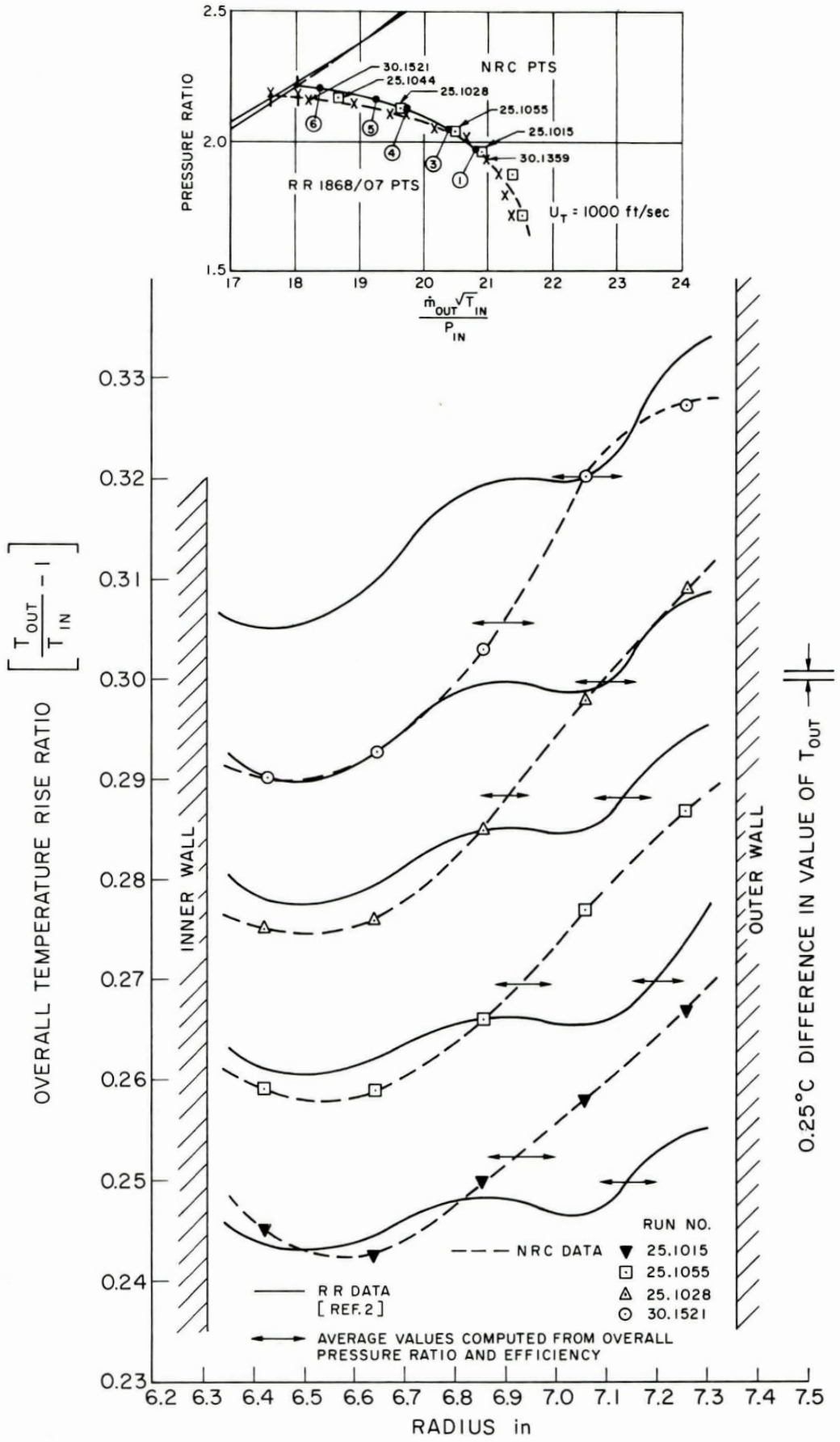

FIG. 16 : OUTLET TOTAL TEMPERATURE PROFILES — U_T = 1000 ft/sec

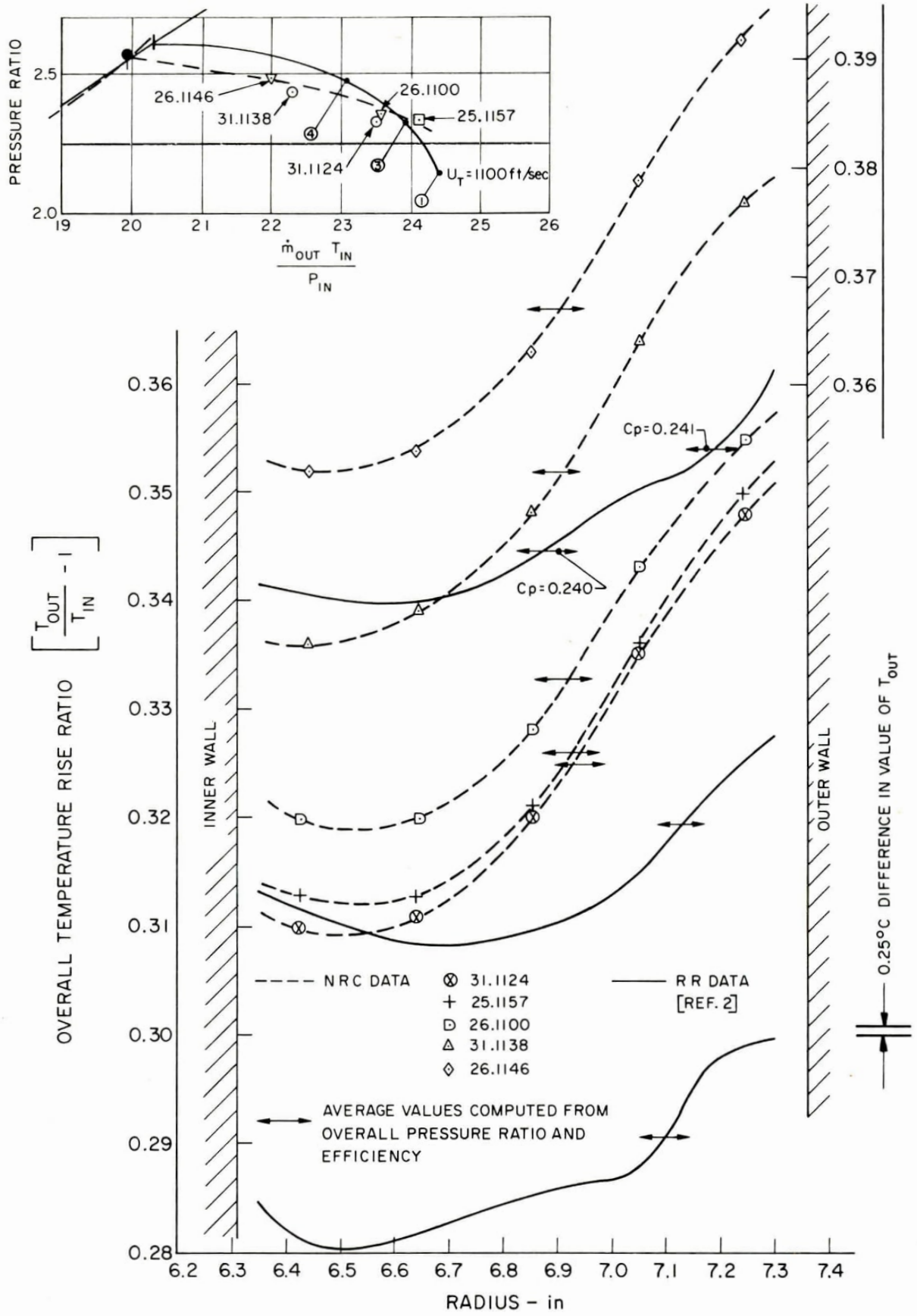

FIG.17 : OUTLET TOTAL TEMPERATURE PROFILES — U_T = 1100 ft/sec

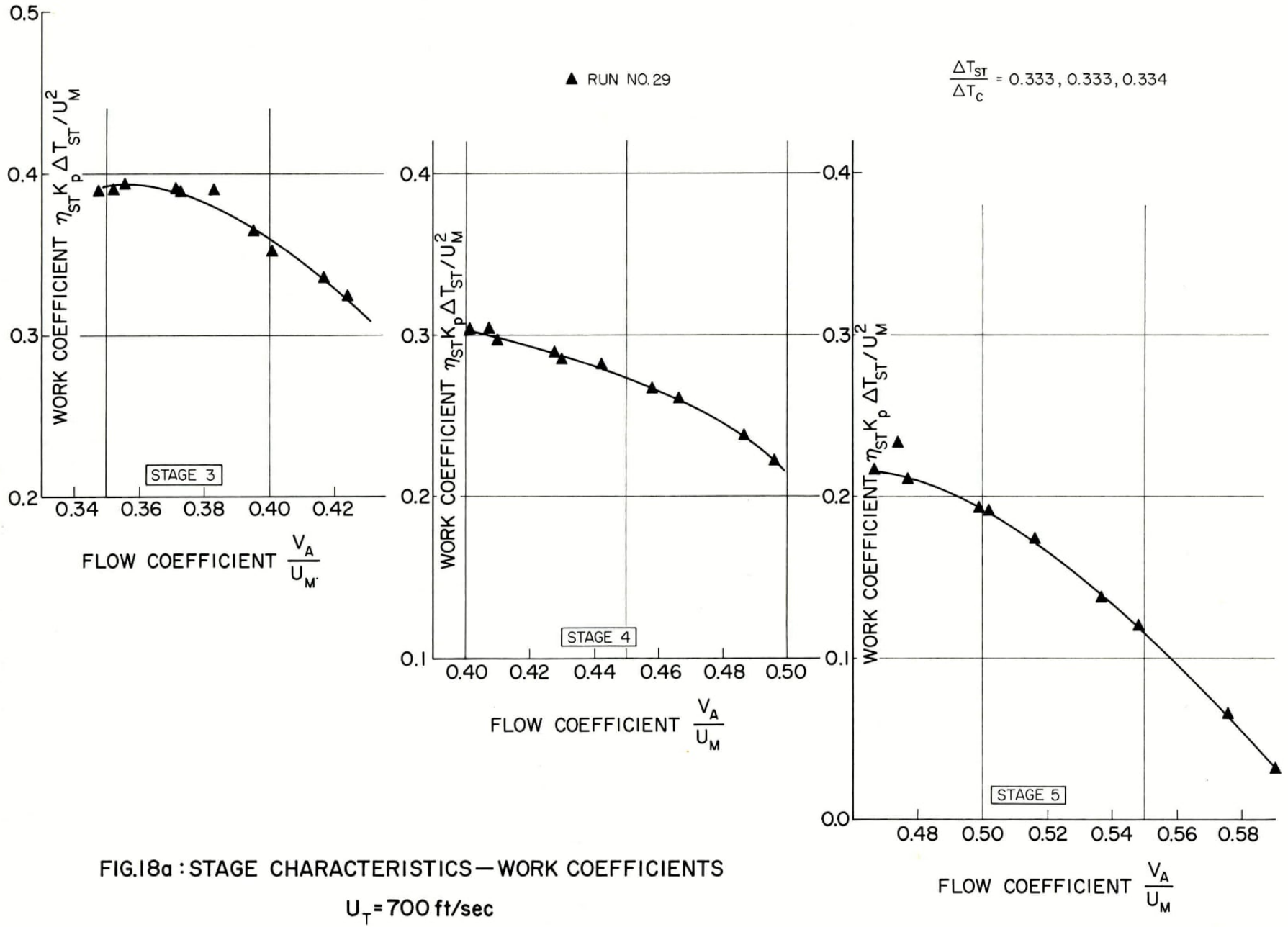

FIG.18a : STAGE CHARACTERISTICS — WORK COEFFICIENTS

U_T = 700 ft/sec

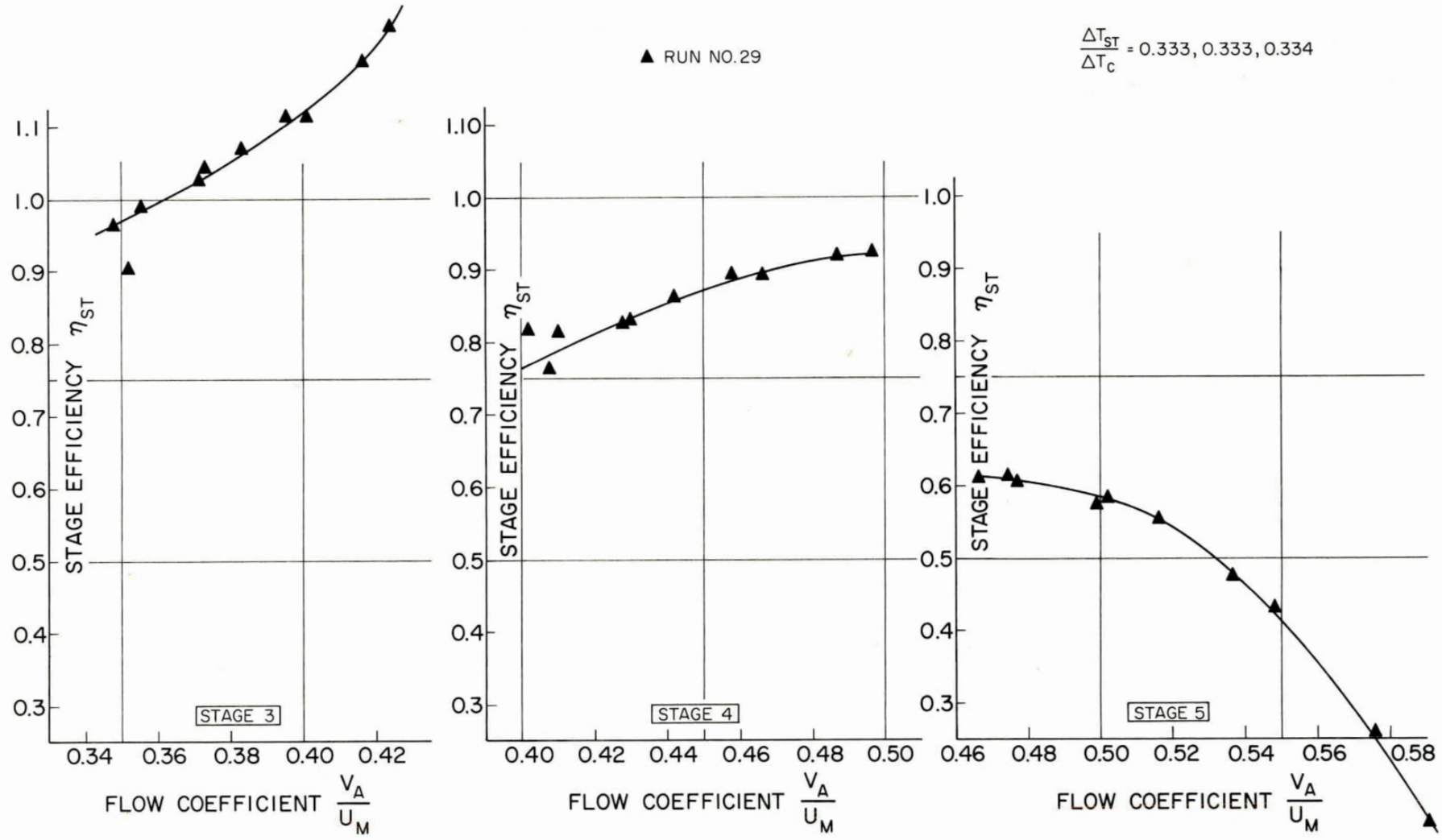

FIG. 18 b : STAGE CHARACTERISTICS – STAGE EFFICIENCIES U_T = 700 ft/sec

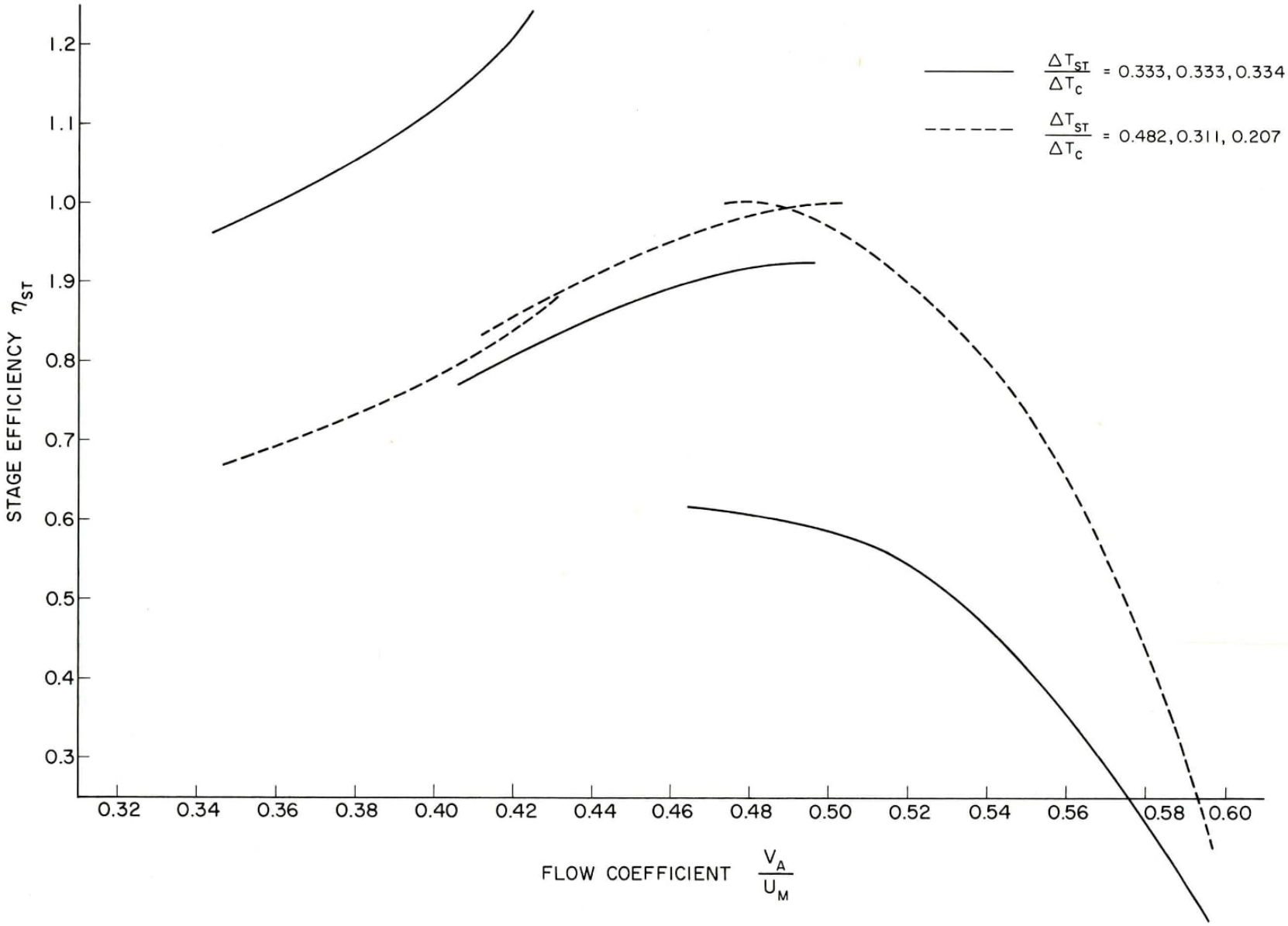

FIG.18c : COMPOSITE STAGE CHARACTERISTICS — STAGE EFFICIENCIES U_T = 700 ft/sec

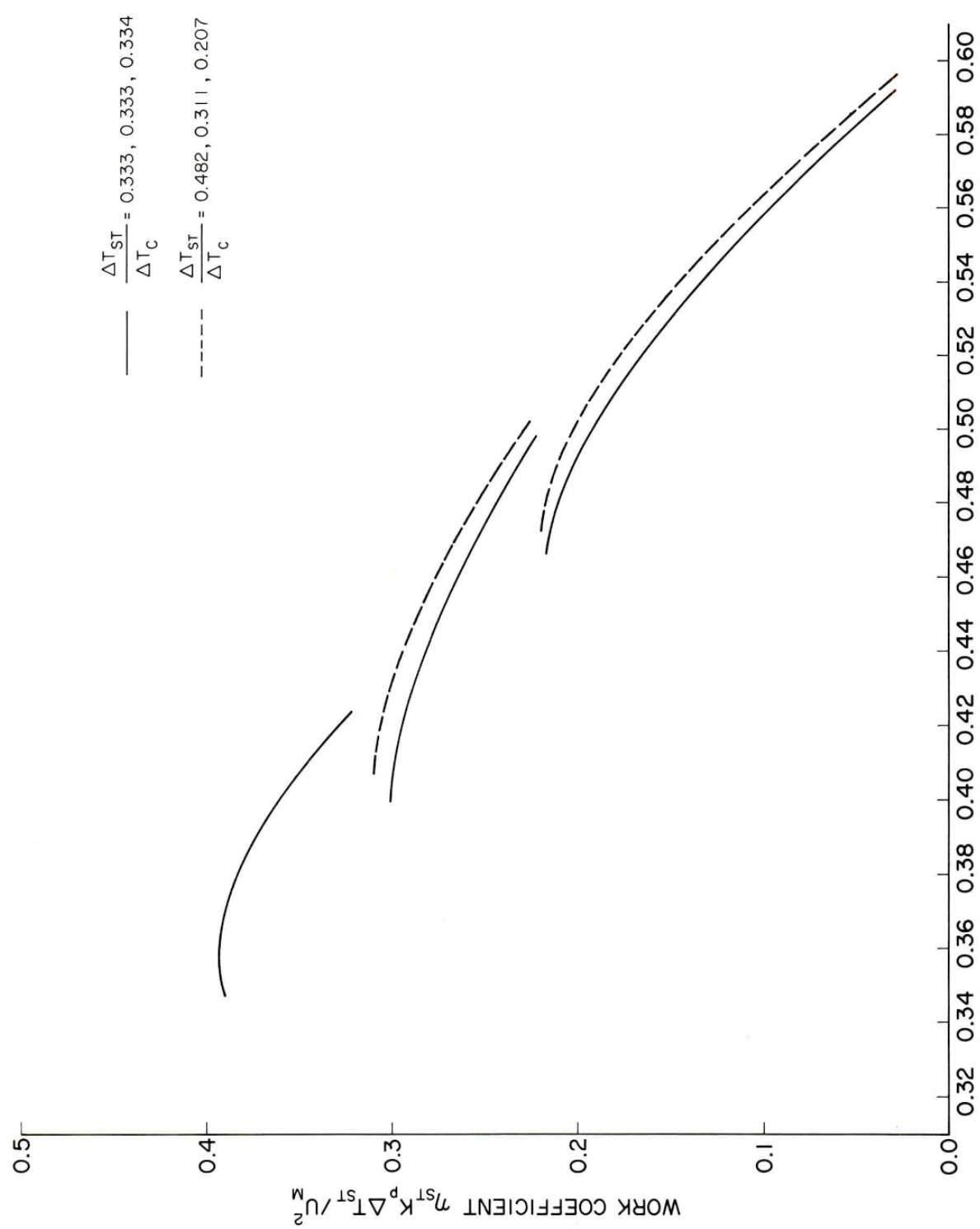

FIG. 18 d: COMPOSITE STAGE CHARACTERISTICS – WORK COEFFICIENTS U_T = 700 ft/sec

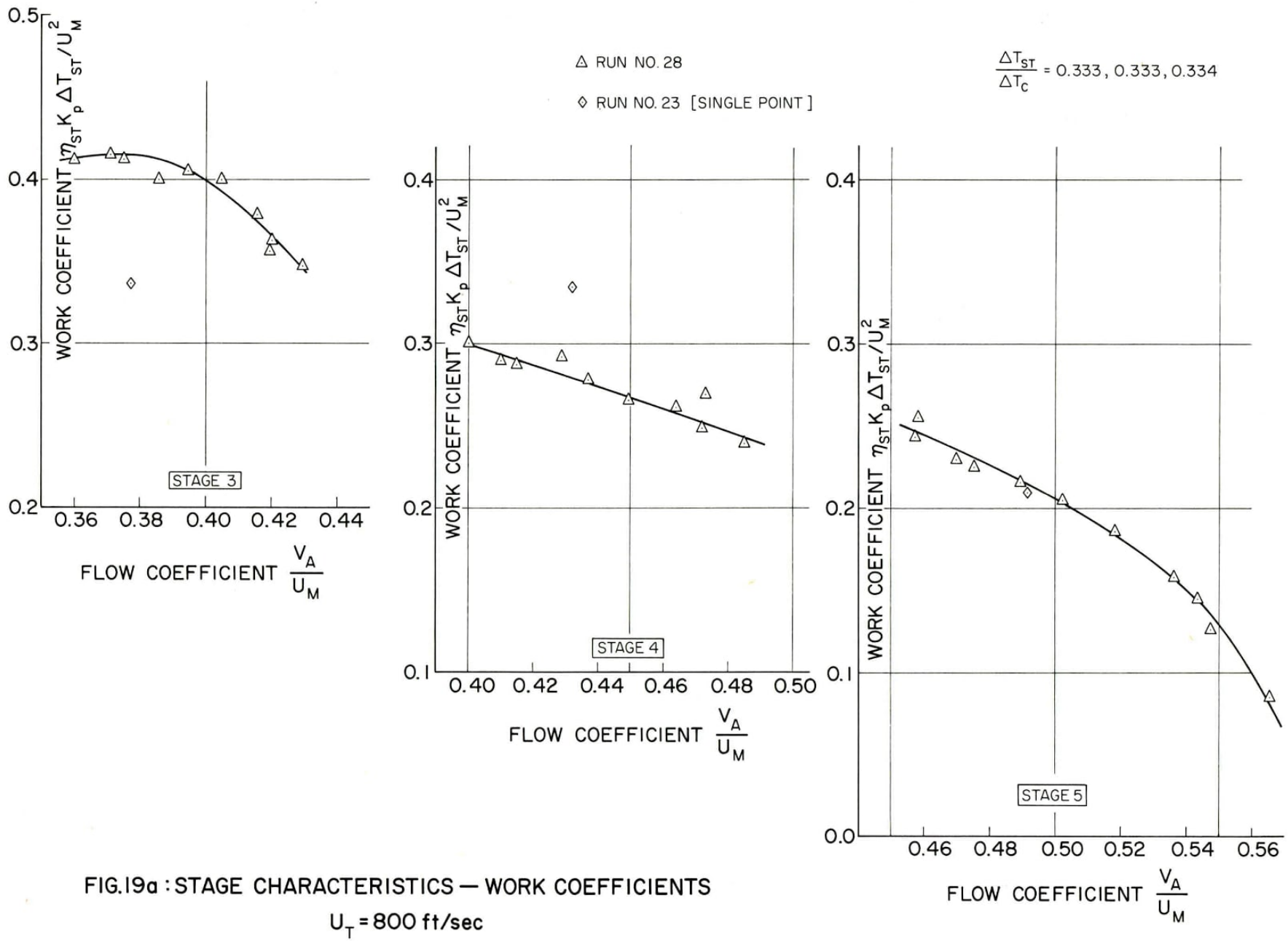

FIG.19a : STAGE CHARACTERISTICS — WORK COEFFICIENTS

U_T = 800 ft/sec

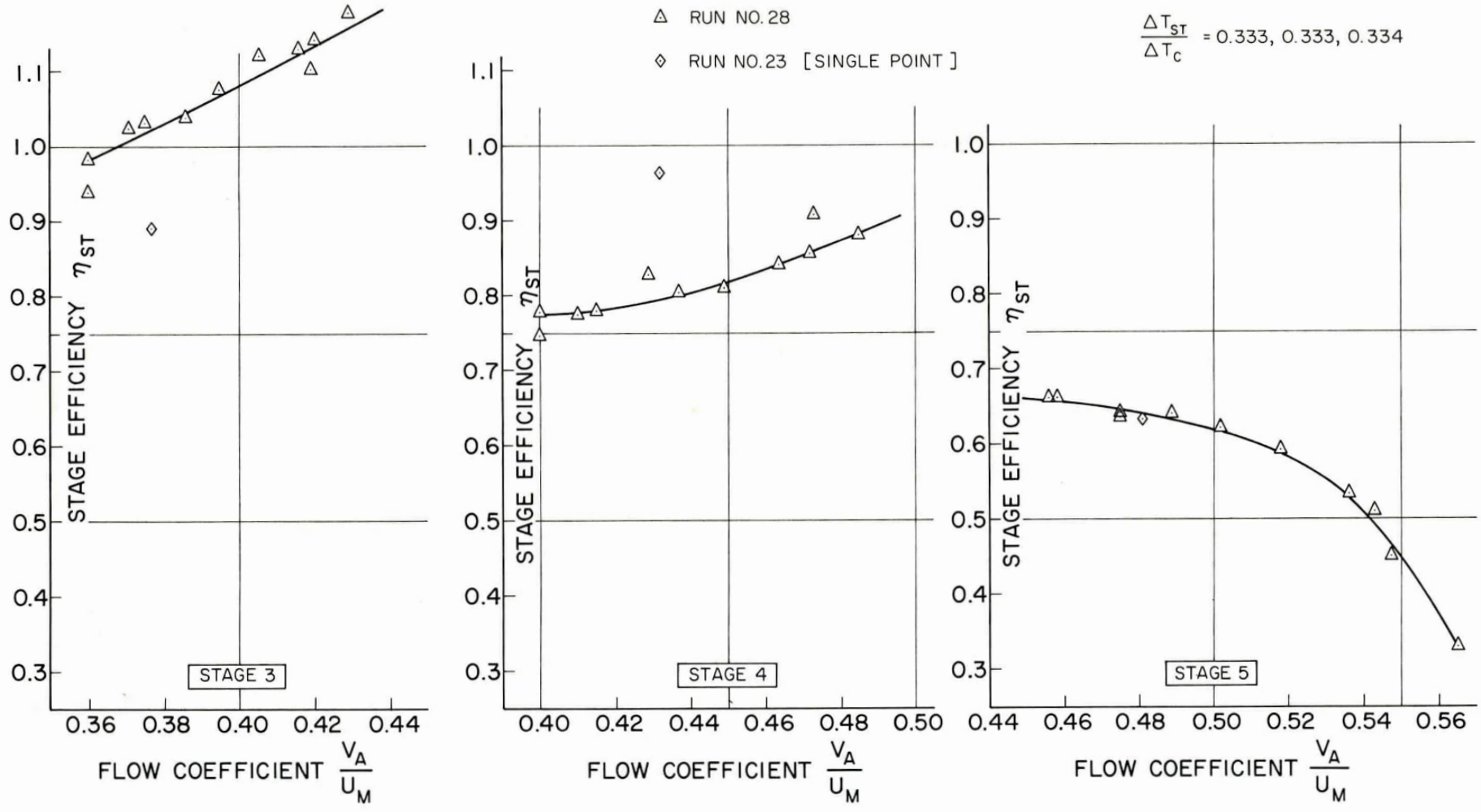

FIG. 19b : STAGE CHARACTERISTICS — STAGE EFFICIENCIES U_T = 800 ft/sec

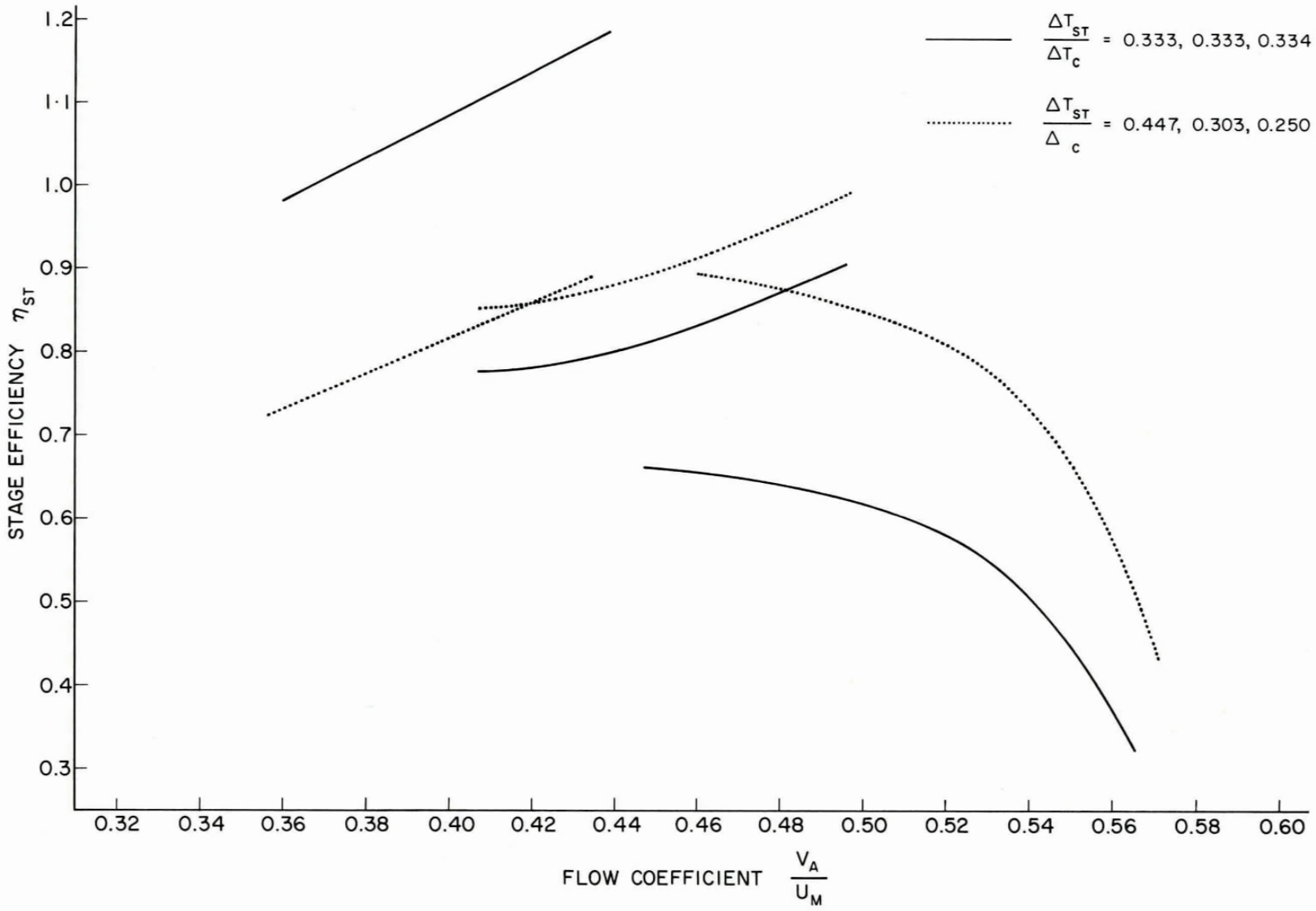

FIG. 19c : COMPOSITE STAGE CHARACTERISTICS — STAGE EFFICIENCIES U_T = 800 ft/sec

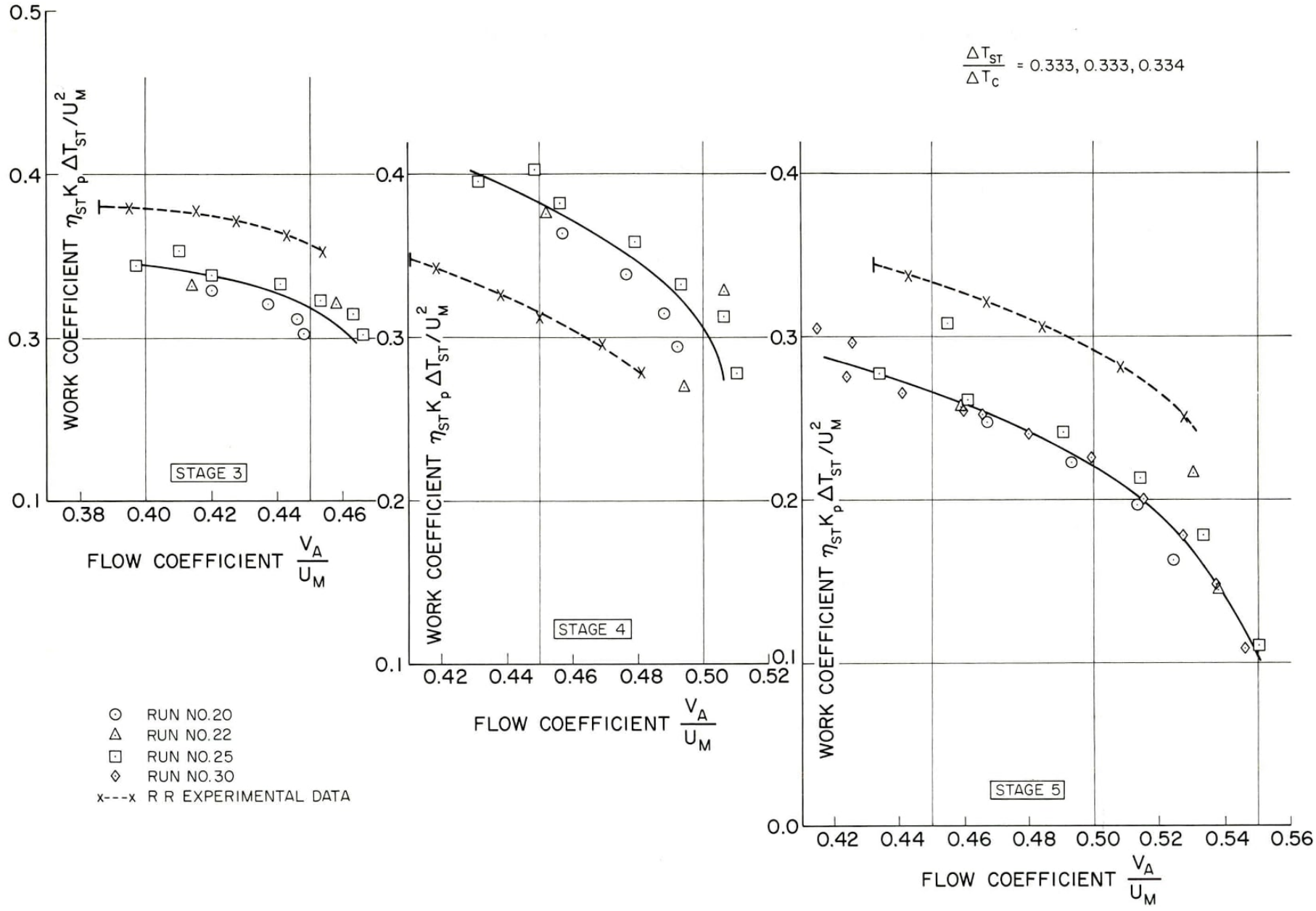

FIG.20a : STAGE CHARACTERISTICS — WORK COEFFICIENTS U_T = 1000 ft/sec

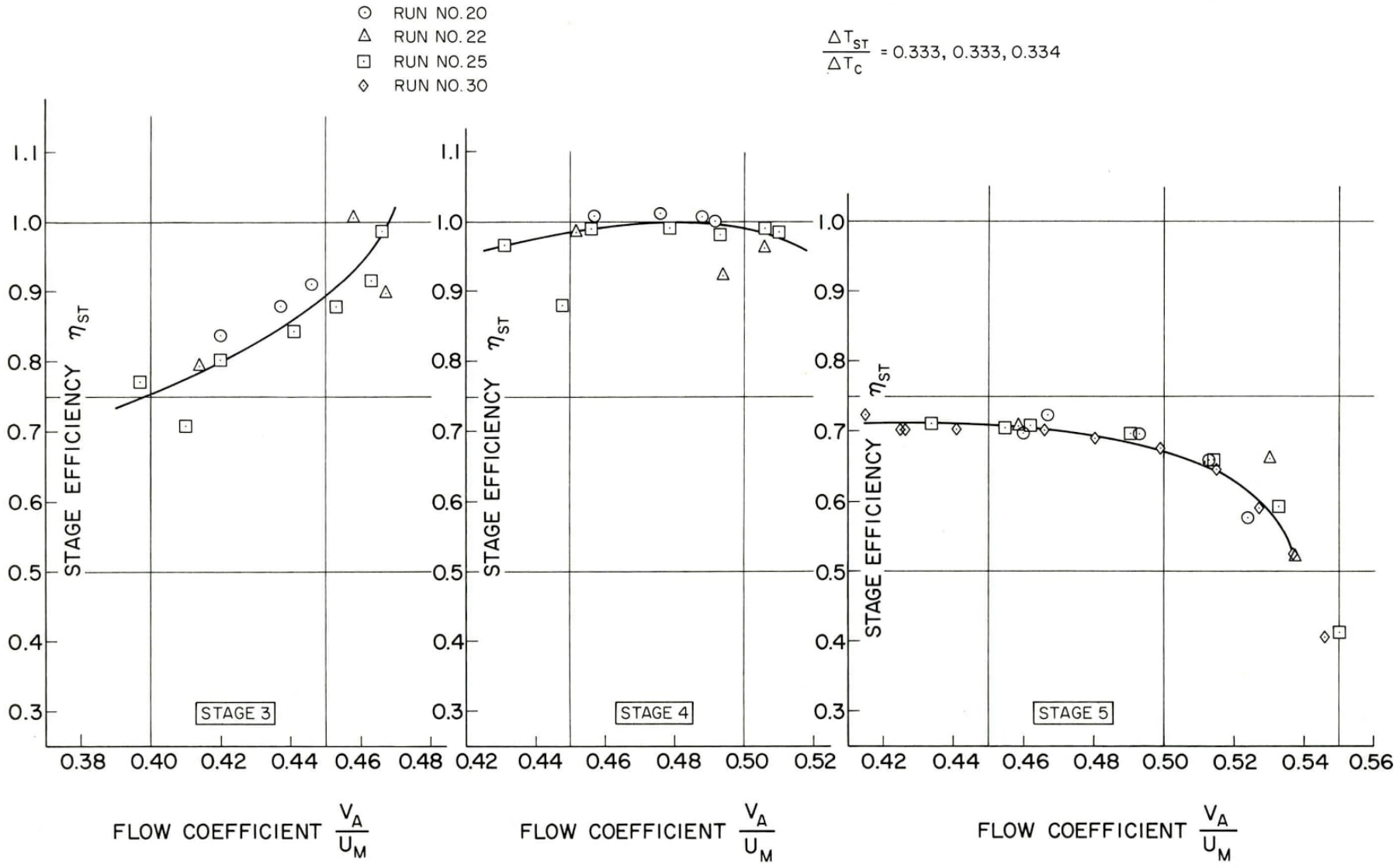

FIG. 20b : STAGE CHARACTERISTICS – STAGE EFFICIENCIES U_T = 1000 ft/sec

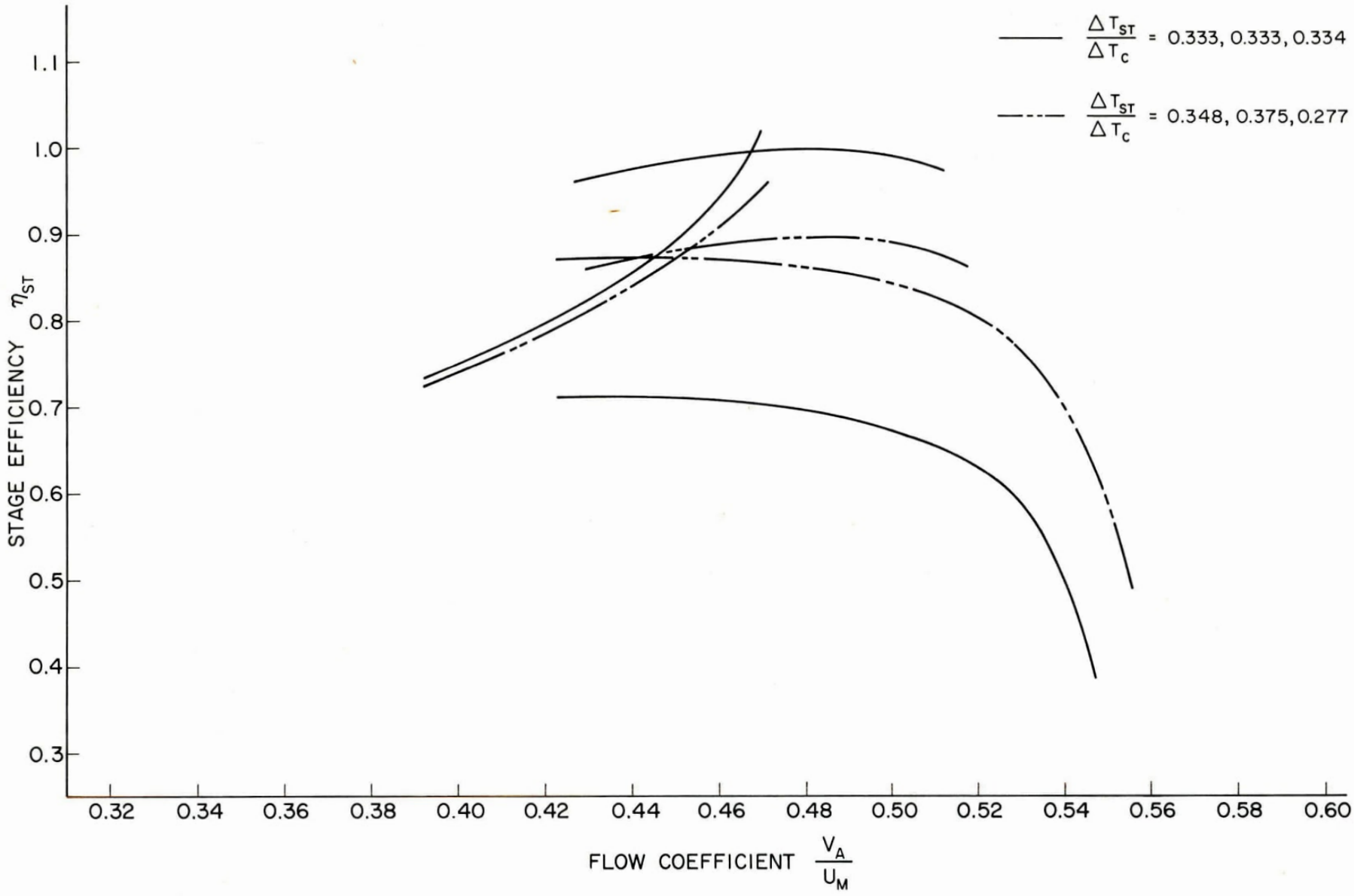

FIG.20c : COMPOSITE STAGE CHARACTERISTICS — STAGE EFFICIENCIES U_T = 1000 ft/sec

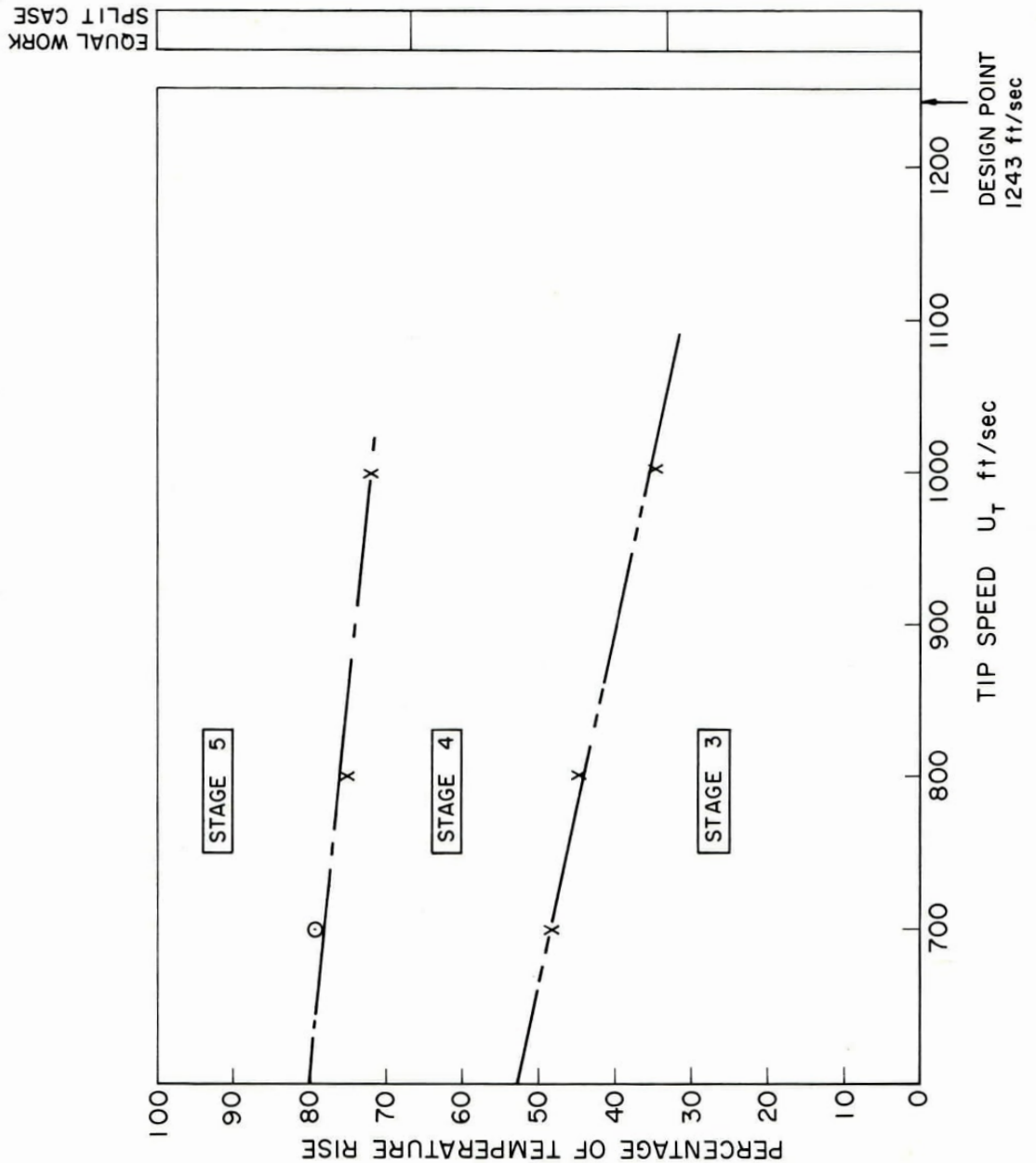

FIG. 21 : STAGE CHARACTERISTICS — DERIVED WORK SPLITS vs TIP SPEED

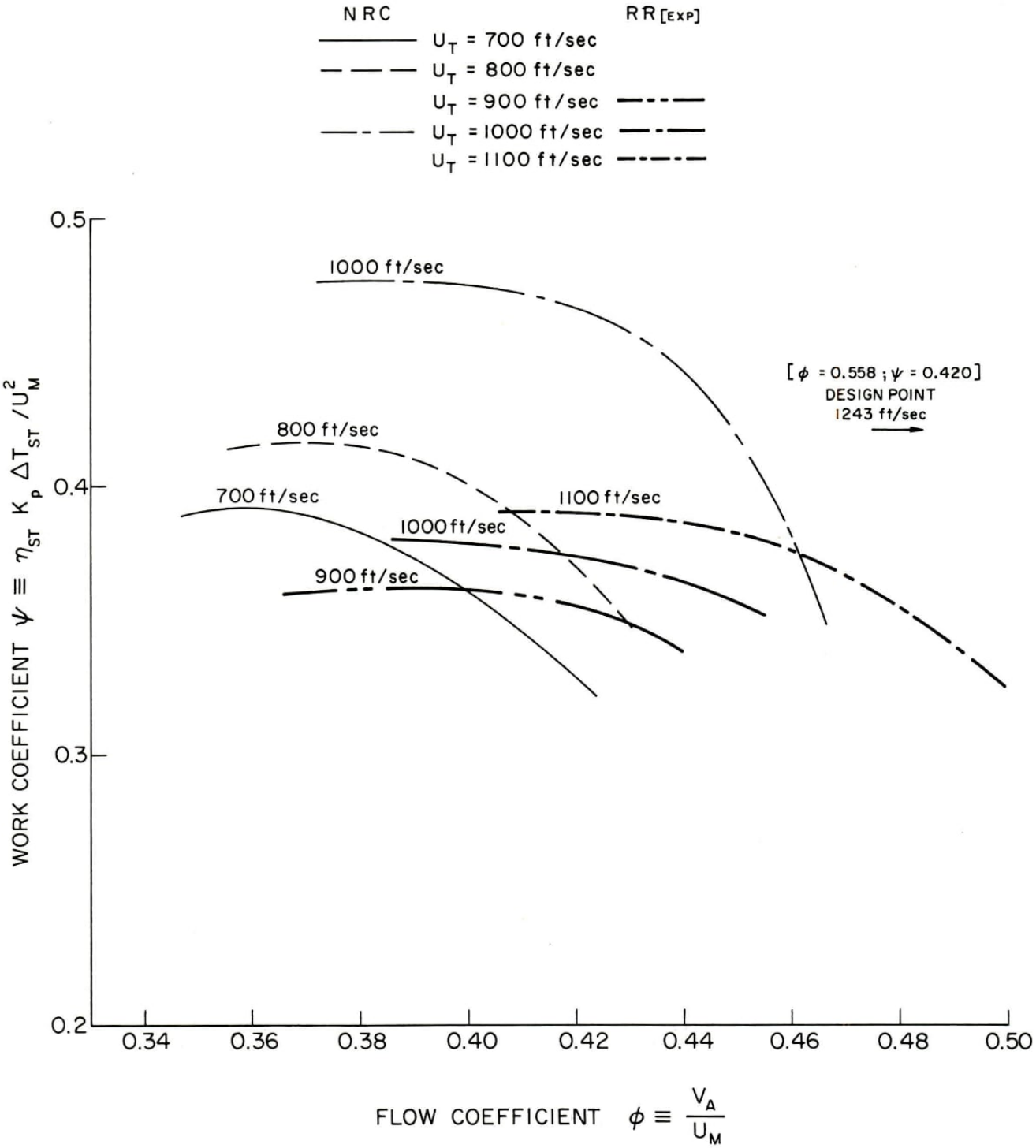

FIG. 22a : STAGE CHARACTERISTICS — STAGE 3 WORK COEFFICIENTS

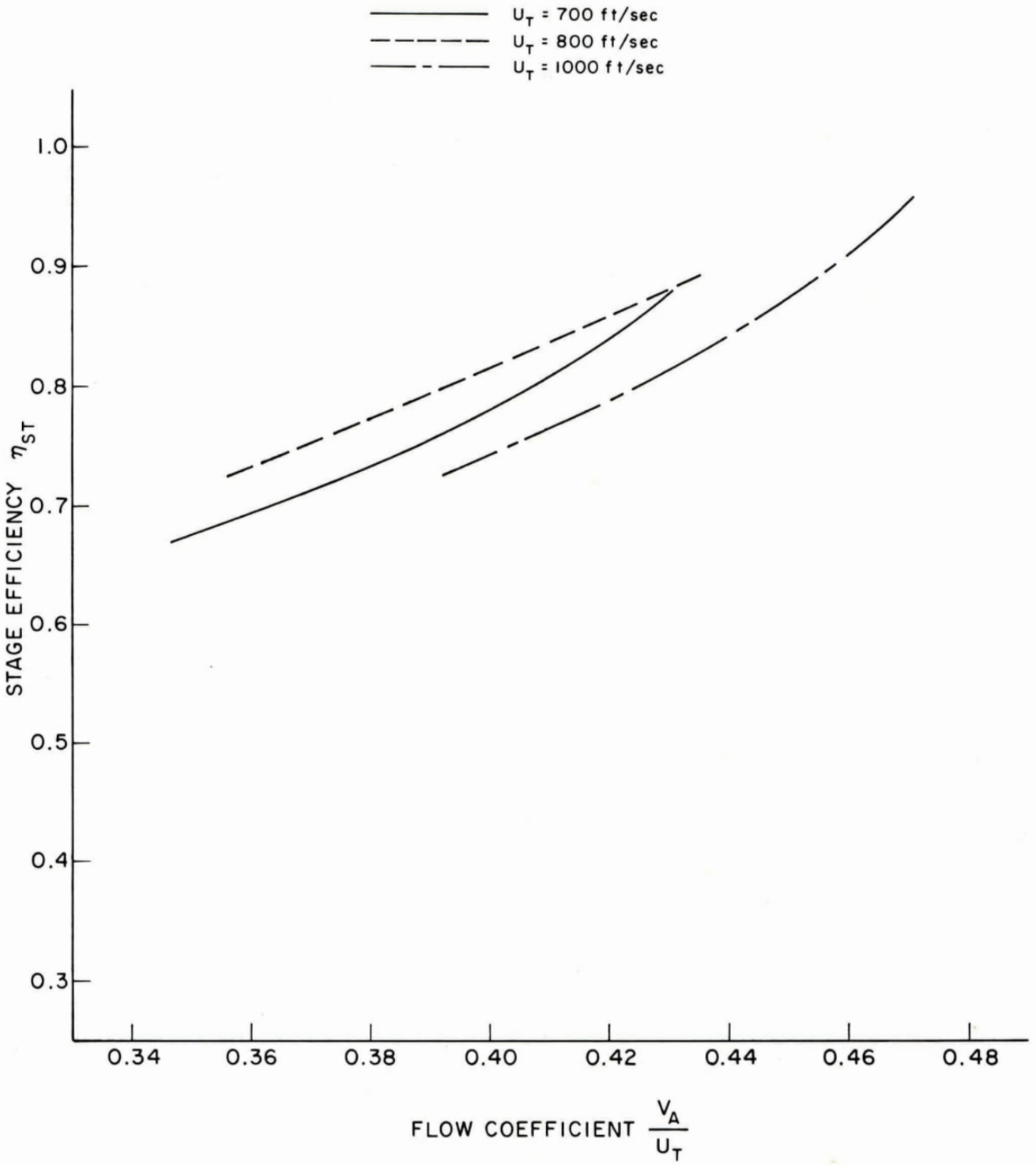

FIG. 22b : STAGE CHARACTERISTICS — STAGE 3 EFFICIENCIES

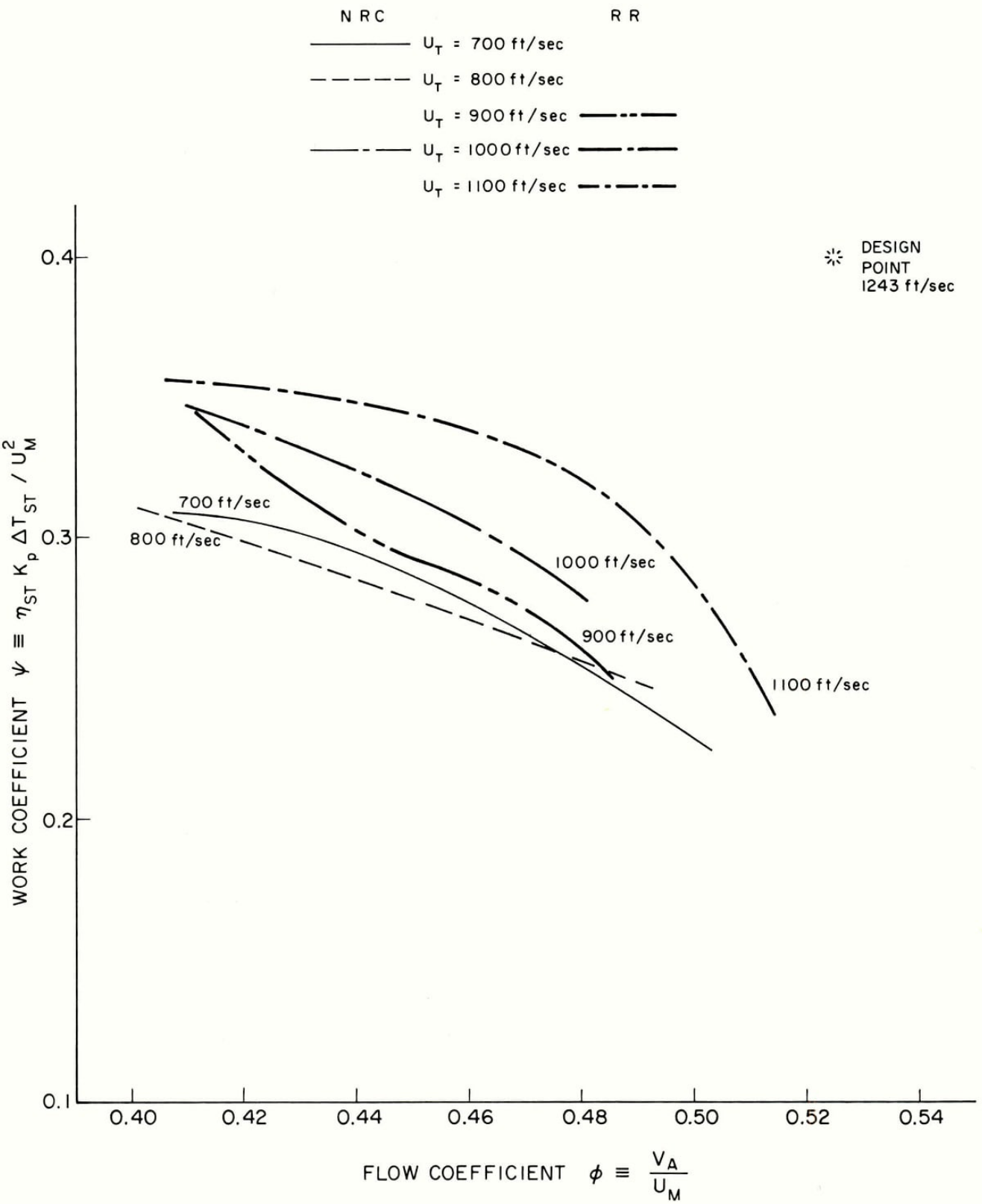

FIG. 23a : STAGE CHARACTERISTICS — STAGE 4 WORK COEFFICIENTS

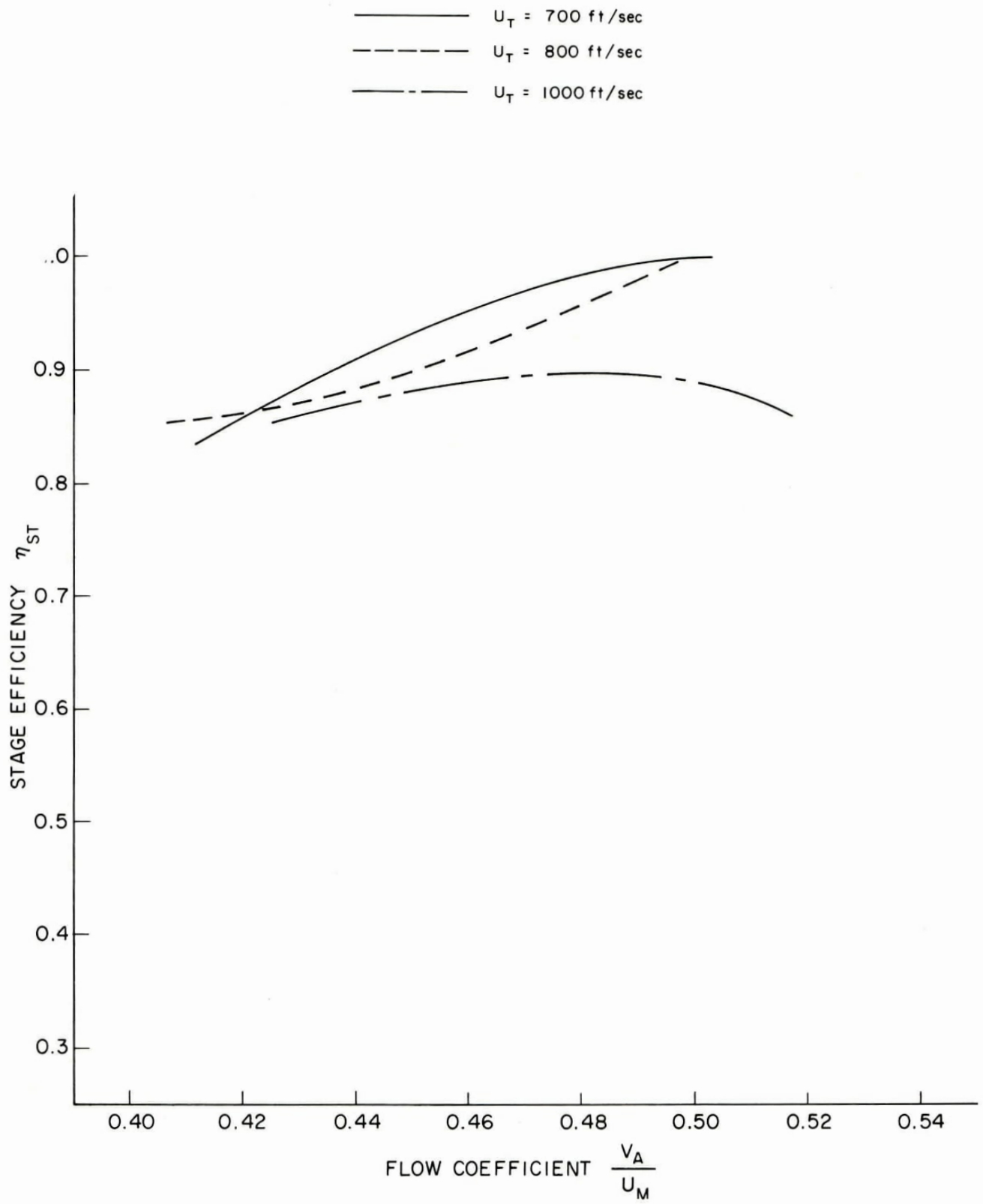

FIG. 23b : STAGE CHARACTERISTICS — STAGE 4 EFFICIENCIES

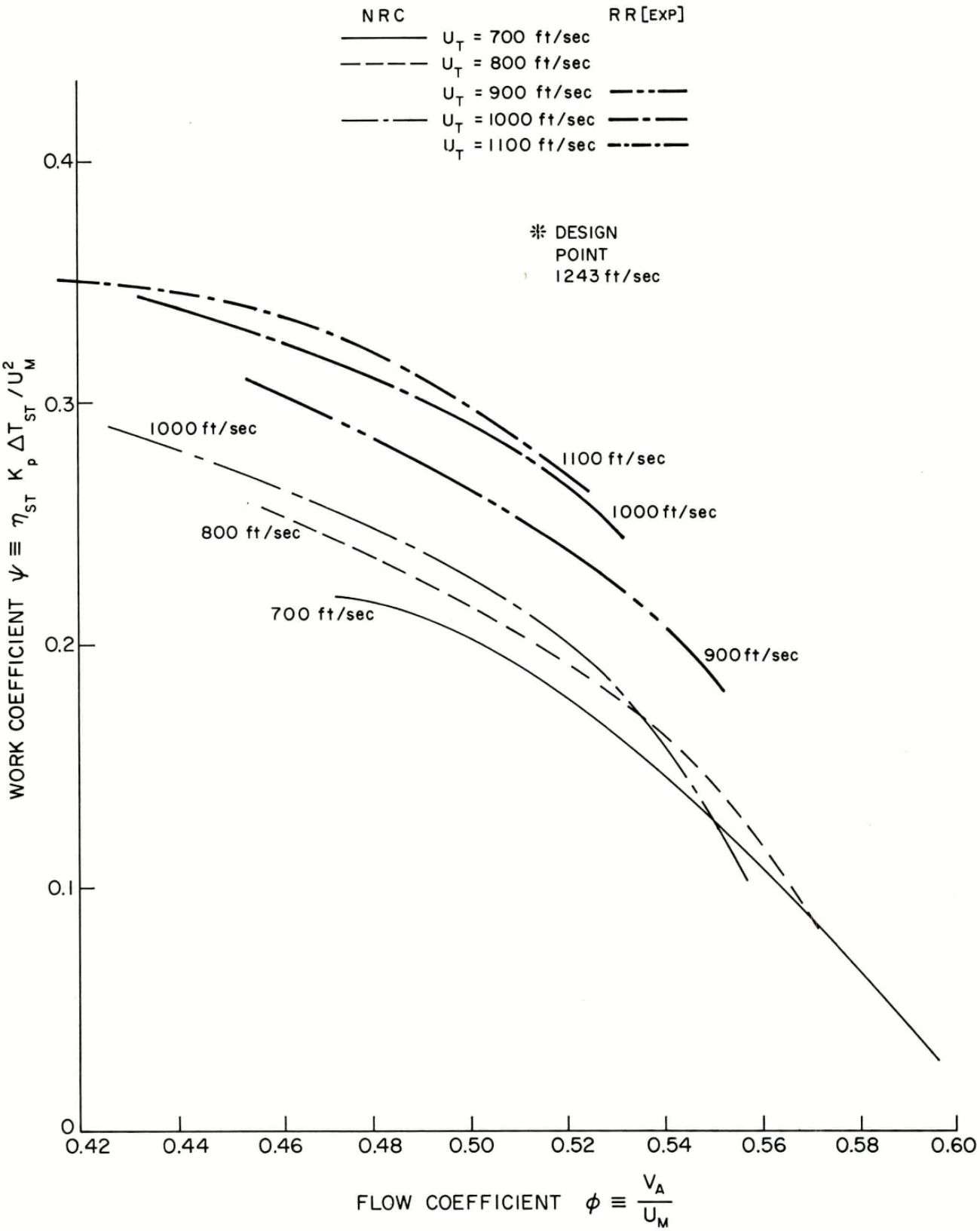

FIG. 24a : STAGE CHARACTERISTICS — STAGE 5 WORK COEFFICIENTS

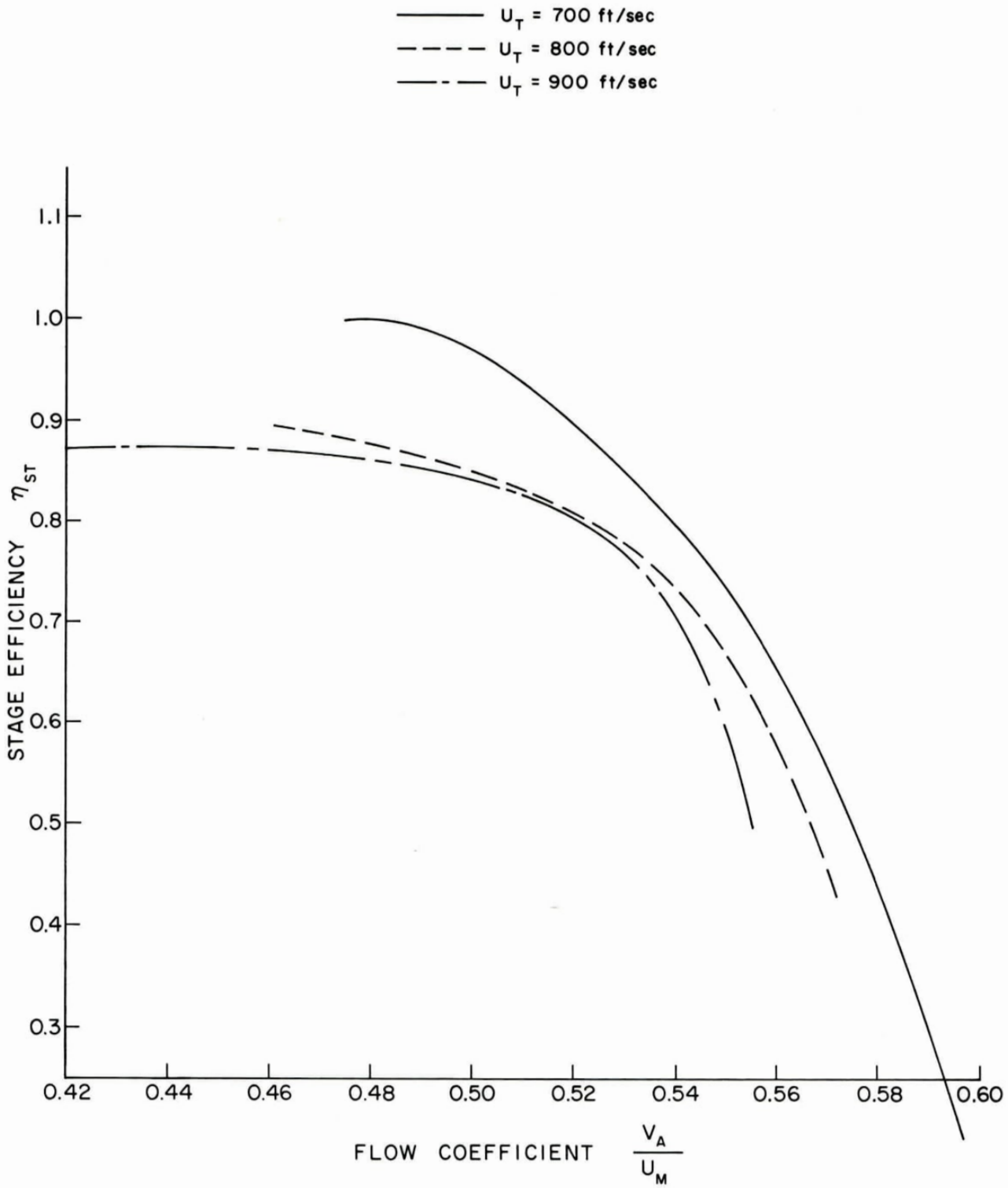

FIG. 24b : STAGE CHARACTERISTICS — STAGE 5 EFFICIENCIES

APPENDIX A

GEOMETRIC DETAILS OF AIRPATH AND COMPRESSOR BLADING

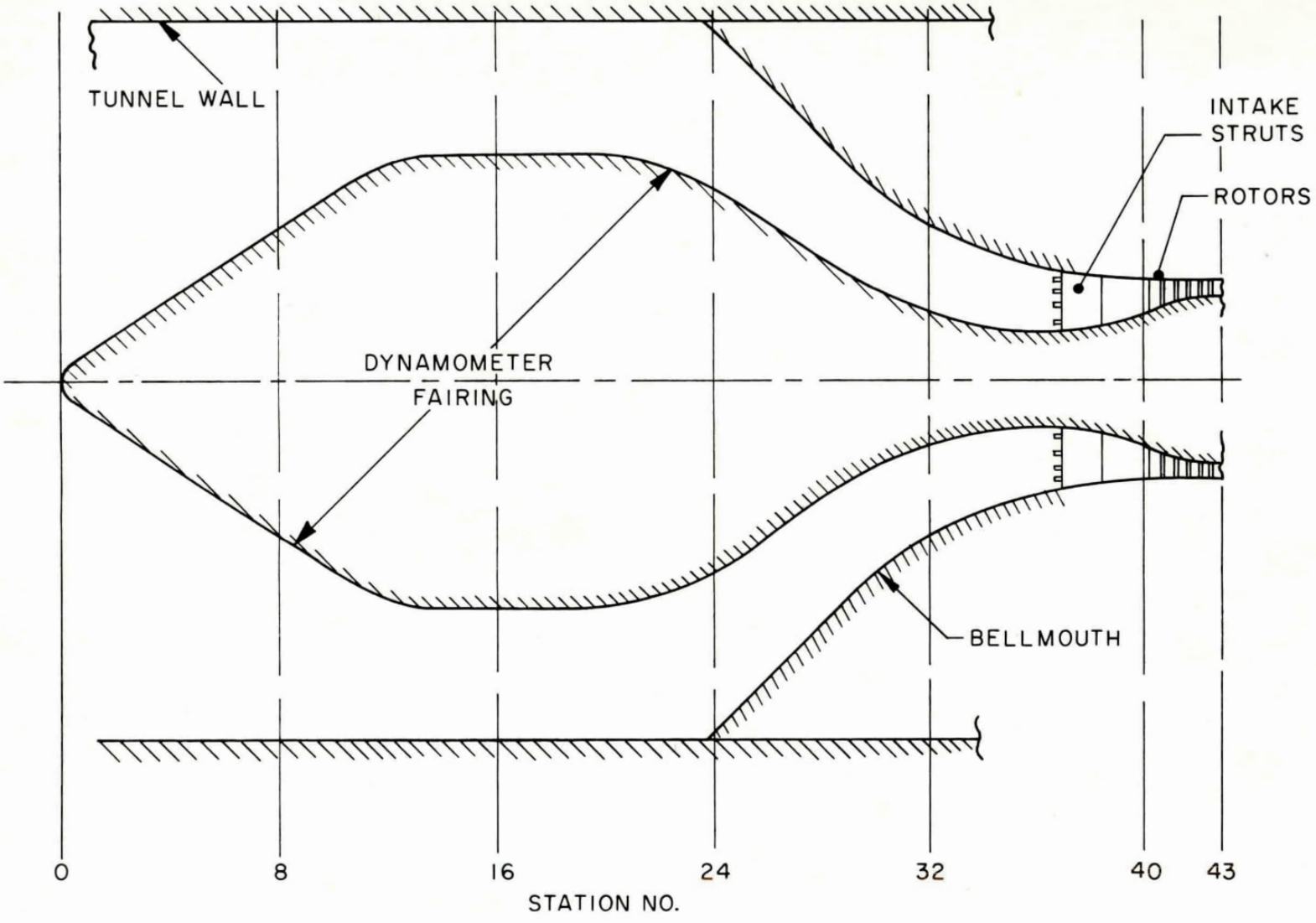

FIG. A-1a : COMPRESSOR INTAKE AIRPATH

STATION NO.	STATION INCHES	INSIDE DIAMETER INCHES	OUTSIDE DIAMETER INCHES
0	0	0.00	53.75
1	2	4.77	53.75
2	4	7.37	53.75
3	6	9.96	53.75
4	8	12.56	53.75
5	10	15.16	53.75
6	12	17.76	53.75
7	14	20.36	53.75
8	16	22.95	53.75
9	18	25.55	53.75
10	20	28.15	53.75
11	22	30.78	53.75
12	24	32.63	53.75
13	26	33.66	53.75
14	28	34.00	53.75
15	30	34.00	53.75
16	32	34.00	53.75
17	34	34.00	53.75
18	36	34.00	53.75
19	38	34.00	53.75
20	40	33.98	53.75
21	42	33.53	53.75
22	44	32.50	53.75
22.5	45	31.74	53.75
23	46	30.80	53.75
23.5	47	29.90	53.75
24	48	28.85	52.44
24.5	49	27.67	50.44
25	50	26.41	48.44
25.5	51	25.14	46.44
26	52	23.81	44.44
26.5	53	22.47	42.44
27	54	21.08	40.44
27.5	55	19.69	38.44
28	56	18.33	36.44
28.5	57	17.03	34.44
29	58	15.82	32.48
29.5	59	14.68	30.65
30	60	13.61	28.97
30.5	61	12.64	27.42
31	62	11.73	26.02
31.5	63	10.95	24.72
32	64	10.25	23.52
32.5	65	9.60	22.44
33	66	8.99	21.43
33.5	67	8.49	20.52
34	68	8.03	19.69
35	70	7.40	18.27
36	72	7.03	17.15
37	74	7.00	16.32
L. E. Strut	76.293	7.124	15.667
T. E. Strut	79.293	8.092	15.406
Rear Edge Strut Platform Front Edge	80.032	8.331	15.338
R. I. G. V. Platform Rear Edge	81.180	9.065	15.221
R. I. G. V. Platform	82.602	9.988	15.047
L. E. 3R	82.990	10.224	14.999

FIG. A – 1b : COMPRESSOR INTAKE AIRPATH

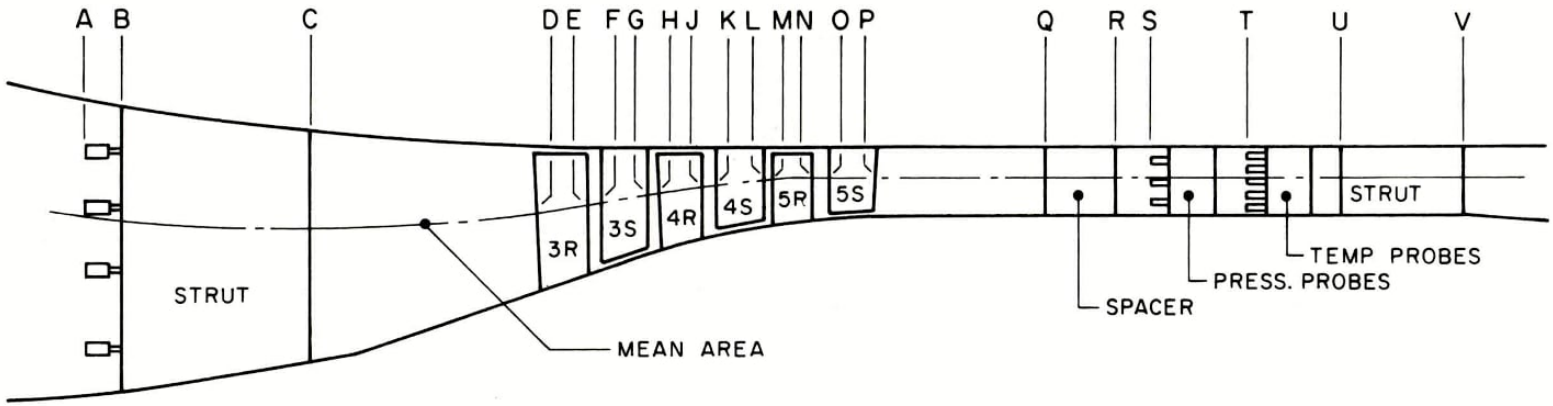

FIG. A-2a : PHASE ZERO TEST COMPRESSOR — AIRPATH

AXIAL STATION	AXIAL DIMENSION	INNER DIAMETER	OUTER DIAMETER	ANNULUS AREA
A	75.71	7.01	15.78	156.98
B	76.29	7.12	15.67	153.04
C	79.29	8.09	15.41	135.10
D	82.99	10.22	15.00	94.68
E	83.74*	10.66*	14.91*	85.35
F	84.00	10.85	14.94	82.84
G	84.81	11.29	14.89	74.02
H	84.95	11.44	14.88	71.11
J	85.61*	11.69*	14.81*	64.94
K	85.86	11.80	14.83	63.37
L	86.55	12.07	14.79	57.38
M	86.72	12.15	14.79	55.63
N	87.37*	12.33*	14.77*	51.93
O	87.58	12.40	14.75	50.11
P	88.30	12.58	14.71	45.65
Q	91.11	12.62	14.71	44.86
R	92.21	12.62	14.71	44.86
S	92.90	12.62	14.71	44.86
T	94.43	12.62	14.71	44.86
U	110.53	12.62	14.71	44.86
V	112.53	12.62	14.71	44.86

NOTE: All Dimensions in Inches
Dimensions indicated thus * were scaled

FIG. A-2b : PHASE ZERO TEST COMPRESSOR — AIRPATH

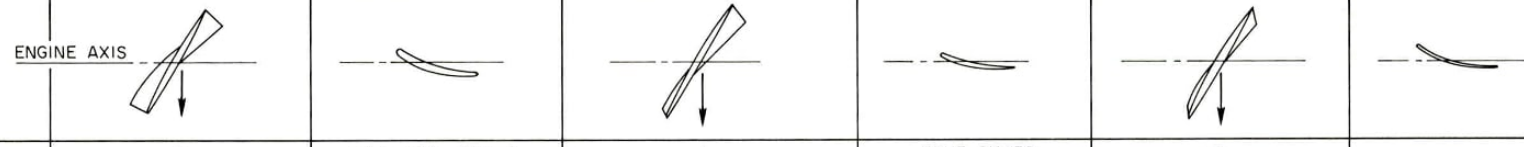

ROTOR STAGE		3				THICKNESS CHORD				4				TRUE CHORD				5						
STATOR STAGE						3								4								(OGV STATOR)		
		I°	O°	+/C%	TRCHD	I°	O°	+/C%	TRCHD	I°	O°	+/C%	TRCHD	I°	O°	+/C%	TRCHD	I°	O°	+/C%	TRCHD	I°	O°	+/C%	TRCHD
SECTION RADIUS	8.0	64.4	61.0	2.95	1.1223	32.8	- 9.0	9.16	0.8139															
"	7.5	62.5	58.4	4.5		34.4	- 9.0	8.13		63.5	57.3	3.96	1.2359	34.0	- 8.5	8.28	0.7162	63.3	56.4	3.55	1.2280	33.9	- 9.2	8.45	0.7469
"	7.0	60.2	54.8	6.05		36.0	- 9.2	7.10		61.7	53.2	4.78	1.1946	35.0	- 8.6	6.88		61.8	52.3	5.87	1.1635	35.1	- 9.3	6.65	
"	6.5	58.0	50.2	7.59	CONSTANT	37.7	- 9.7	6.07	CONSTANT	59.5	48.3	6.13	1.1583	36.75	- 9.0	5.48	CONSTANT	60.0	47.0	8.20	1.0946	36.6	- 9.65	4.85	CONST
"	6.0	55.3	43.8	9.14		39.5	-10.1	5.04		57.2	41.5	8.43	1.1213	39.0	- 9.7	4.08		58.0	39.8	10.52	1.0228	38.6	-10.2	3.05	0.7469
"	5.5	52.5	35.4	10.69		41.6	-10.8	4.01		54.5	32.5	15.0	1.0806	42.25	-10.75	2.68	0.7162								
"	5.0	49.7	22.2	12.24	1.1223	43.8	-11.6	2.98	0.8139																
"	4.5																								
ASPECT RATIO		1.779				2.034				1.422				2.025				1.138				1.501			
FORM		LENTICULAR-ET 7306 ADC1777				C4 MOD4 ADC 2219				LENTICULAR-ET 7306 ADC 1777				C4 MOD 5 ADC 2219				LENTICULAR-ET 7306 ADC1777				C4 MOD 5 ADC 2219			
NO. OFF		53				88				41				100				41				88			
AXIAL LEAN, IN/IN		0.010								0.012								0.013							
TANGENTIAL LEAN, IN		0.0052								0.0051								0.0054							
TOTAL CIRCUMFER^{L}CLEAR^{CE}		0.020 + 0.020				0.030 + 0.020				0.020 + 0.020				0.060 + 0.020				0.020 + 0.020				0.080 + 0.020			
RADIAL GROWTH	DISC THERMAL Δ	0.0051								0.0073								0.0098							
	DISC CF Δ	0.0051								0.0072								0.0066							
	BLADE THERMAL Δ	0.0041				0.0040				0.0046				0.0037				0.0045				0.0038			
	BLADE CF Δ	0.0035								0.0024								0.0018							

FIG. A-3 : PHASE ZERO TEST COMPRESSOR — AIRFOIL DATA

APPENDIX B

SAMPLE OUTPUT SHEETS

OVERALL AND STAGE PERFORMANCE PARAMETERS

SMALL COMPRESSOR UNIT - PHASE ZERO

REDUCED EXPERIMENTAL RESULTS

BARO. 30.121 INHG

PROCESSED FEB. 5 1970

** INPUT DATA **

RUN NO.	30.1359
BARO	1020.0
RRPM	15465
TO 1	22.90
TO 2	22.00
TO 3	21.40
TO 4	21.00
T7YP3	96.00
T8 1	97.80
T8 2	95.30
T8 3	92.90
T8 4	91.10
T8 5	91.30
PVT	71.50
SVT	72.90
PVEA	73.00
SVEA	75.80
PO 0	12.50
PO 1	7.92
PO 1	21.98
PO 2	21.95
PO 3	22.02
PO 4	22.01
ZEROA	80.11
P3R	80.67
P3S	75.98
P4R	72.42
P4S	66.61
P5R	65.29
P5S	58.76
P6	60.20
YPA3	2/27/40.0
ZEROB	80.16
P7 3	51.08
P8 0	59.80
P8 1	59.76
P8 1	52.71
P8 2	51.12
P8 3	52.12
PVPU	14.85
PVSU	19.10
PVPDIFF	2.75
PVSDIFF	16.90

STATION		TOTAL PRESSURE INHG ABS	STATIC PRESSURE INHG ABS	TOTAL TEMPERATURE DEG C	MASS FLOWRATE LBM/SEC	
INTAKE (OBSERVED)		30.27	29.37	20.2	19.14	DELTA 1.01161
					(19.09)C	THETA 1.01795
					AVG.(19.09)	
INTERSTAGE STATICS						PRESSURE RATIO
	R RIGV - 3R		29.22			0.977
	E 3R - 3S		33.86			1.132
	D 3S - 4R		37.38			1.249
	U 4R - 4S		43.12			1.441
	C 4S - 5R		44.43			1.485
	F 5R - 5S		50.88			1.701
	D TE OF 5S		49.46			1.653
YAW PROBE DATA (REDUCED)		58.52		87.3	AT FLOW ANGLE OF + 2.33 DEG	
LEAKAGE VENTURIS						
(OBSERVED)	PORT			70.8	0.03	
(DATA)	STBD			73.6	0.08	DATA AT UPPER LIMIT MASS FLOW DISCREPANCY -5.0 PERCENT
OUTLET (REDUCED)		57.63	50.50	85.0	18.58	
					(18.63)D	

*** MAJOR PERFORMANCE DATA ***

REDUCED SPEED	15328	R.P.M.
PRESSURE RATIO	1.926	
REDUCED OUTLET MASS FLOW	18.131	LBM/SEC
(M ROOT T ON P)	20.944	
TEMPERATURE EFFICIENCY	84.79	PERCENT

PROCESSED FEB. 5 1970

SMALL COMPRESSOR UNIT - PHASE ZERO

STAGE CHARACTERISTICS

MEAN FLOW ANGLE (DEG)	MEAN RADIUS (IN)	ANNULUS AREA (SQ IN)	STATIC PRESSURE (INHG ABS)	STATION	STAGE EFFICIENCY	COEFFICIENTS FLOW	COEFFICIENTS WORK	PRESSURE RATIOS ROW	PRESSURE RATIOS STAGE
0.0	6.3060	94.620	29.22	RIGV - 3R				0.977 (0.920)	
						0.4540			
******	6.5770	71.200	33.86	3R - 3S				1.132	1.3617
					1.1389		0.4038		
0.0	*******	*******	37.38	3S - 4R				1.249	
						0.4602			
******	6.7330	55.840	43.12	4R - 4S				1.441	1.2120
					0.7540		0.2458		
0.0	*******	*******	44.43	4S - 5R				1.485	
						0.5155			
******	6.8300	45.490	50.88	5R - 5S				1.701	1.1670
					0.6475		0.2014		
0.0	*******	*******	49.46	TE OF 5S				1.653 (1.682)	

ASSUMED WORK SPLIT
0.333, 0.333, 0.333

GAMMA 1.400

REF. TIP RADIUS 7.4995 IN

NOM. TIP SPEED 1003 FT/SEC

****'MAJOR PERFORMANCE DATA ****

REDUCED SPEED	15328	R.P.M.
PRESSURE RATIO	1.926	
REDUCED OUTLET MASS FLOW	18.131	LBM/SEC
(M ROOT T ON P)	20.944	
TEMPERATURE EFFICIENCY	84.79	PERCENT

PROCESSED FEB. 5 1970

SMALL COMPRESSOR UNIT - PHASE ZERO

STAGE CHARACTERISTICS

MEAN FLOW ANGLE (DEG)	MEAN RADIUS (IN)	ANNULUS AREA (SQ IN)	STATIC PRESSURE (INHG ABS)	STATION	STAGE EFFICIENCY	COEFFICIENTS FLOW	COEFFICIENTS WORK	PRESSURE RATIOS ROW	PRESSURE RATIOS STAGE
0.0	6.3060	94.620	29.22	RIGV - 3R				0.977 (0.920)	
						0.4540			
******	6.5770	71.200	33.86	3R - 3S				1.132	1.3621
					1.0919		0.4042		
0.0	*******	*******	37.38	3S - 4R				1.249	
						0.4617			
******	6.7330	55.840	43.12	4R - 4S				1.441	1.2131
					0.6758		0.2478		
0.0	*******	*******	44.43	4S - 5R				1.485	
						0.5214			
******	6.8300	45.490	50.88	5R - 5S				1.701	1.1656
					0.7822		0.2021		
0.0	*******	*******	49.46	TE OF 5S				1.653 (1.682)	

ASSUMED WORK SPLIT
0.348, 0.375, 0.277

GAMMA 1.400

REF. TIP RADIUS 7.4995 IN

NOM. TIP SPEED 1003 FT/SEC

**** MAJOR PERFORMANCE DATA ****

REDUCED SPEED 15328 R.P.M.

PRESSURE RATIO 1.926

REDUCED OUTLET MASS FLOW 18.131 LBM/SEC
(M ROOT T ON P) 20.944

TEMPERATURE EFFICIENCY 84.79 PERCENT

RUN NO. 30.1359
SHEET 2

NRC, DME ME-234
National Research Council of Canada. Division of Mechanical Engineering.

THE ROTATING STATOR CONCEPT: PRELIMINARY CALIBRATION OF THE COMPRESSOR IN THE CONVENTIONAL CONFIGURATION.
M.S. Chappell. July 1970. 75 pp. (incl. tabs. app. and figs.)

The background and objectives of an extensive program of research into a novel concept of co-rotating stator rows within an axial compressor are outlined. The test compressor to be used in the experimental investigations is described in detail, as is the NRC Compressor Test Facility wherein the tests are conducted.

The major portion of this initial report comprises results from the preliminary calibration of the three-stage test compressor operated in the conventional configuration (i.e. with the stator rows stationary). This datum performance run was prematurely terminated by a drive train failure but some useful data were obtained at speeds up to about eighty percent of the design value. These data are compared with results from a previous series of tests on another compressor of the same aerodynamic design. The correlation of overall performance parameters was acceptable, but individual stage characteristics required considerable adjustment to obtain satisfactory agreement with previous results.

UNCLASSIFIED

1. Axial flow compressors - Test results
2. Compressor rotors
3. Turbofan engines
4. Gas Turbines
5. Turbomachinery

I. Chappell, M.S.
II. NRC, DME ME-234

NRC, DME ME-234
National Research Council of Canada. Division of Mechanical Engineering.

THE ROTATING STATOR CONCEPT: PRELIMINARY CALIBRATION OF THE COMPRESSOR IN THE CONVENTIONAL CONFIGURATION.
M.S. Chappell. July 1970. 75 pp. (incl. tabs. app. and figs.)

The background and objectives of an extensive program of research into a novel concept of co-rotating stator rows within an axial compressor are outlined. The test compressor to be used in the experimental investigations is described in detail, as is the NRC Compressor Test Facility wherein the tests are conducted.

The major portion of this initial report comprises results from the preliminary calibration of the three-stage test compressor operated in the conventional configuration (i.e. with the stator rows stationary). This datum performance run was prematurely terminated by a drive train failure but some useful data were obtained at speeds up to about eighty percent of the design value. These data are compared with results from a previous series of tests on another compressor of the same aerodynamic design. The correlation of overall performance parameters was acceptable, but individual stage characteristics required considerable adjustment to obtain satisfactory agreement with previous results.

UNCLASSIFIED

1. Axial flow compressors - Test results
2. Compressor rotors
3. Turbofan engines
4. Gas Turbines
5. Turbomachinery

I. Chappell, M.S.
II. NRC, DME ME-234

NRC, DME ME-234
National Research Council of Canada. Division of Mechanical Engineering.

THE ROTATING STATOR CONCEPT: PRELIMINARY CALIBRATION OF THE COMPRESSOR IN THE CONVENTIONAL CONFIGURATION.
M.S. Chappell. July 1970. 75 pp. (incl. tabs. app. and figs.)

The background and objectives of an extensive program of research into a novel concept of co-rotating stator rows within an axial compressor are outlined. The test compressor to be used in the experimental investigations is described in detail, as is the NRC Compressor Test Facility wherein the tests are conducted.

The major portion of this initial report comprises results from the preliminary calibration of the three-stage test compressor operated in the conventional configuration (i.e. with the stator rows stationary). This datum performance run was prematurely terminated by a drive train failure but some useful data were obtained at speeds up to about eighty percent of the design value. These data are compared with results from a previous series of tests on another compressor of the same aerodynamic design. The correlation of overall performance parameters was acceptable, but individual stage characteristics required considerable adjustment to obtain satisfactory agreement with previous results.

UNCLASSIFIED

1. Axial flow compressors - Test results
2. Compressor rotors
3. Turbofan engines
4. Gas Turbines
5. Turbomachinery

I. Chappell, M.S.
II. NRC, DME ME-234

NRC, DME ME-234
National Research Council of Canada. Division of Mechanical Engineering.

THE ROTATING STATOR CONCEPT: PRELIMINARY CALIBRATION OF THE COMPRESSOR IN THE CONVENTIONAL CONFIGURATION.
M.S. Chappell. July 1970. 75 pp. (incl. tabs. app. and figs.)

The background and objectives of an extensive program of research into a novel concept of co-rotating stator rows within an axial compressor are outlined. The test compressor to be used in the experimental investigations is described in detail, as is the NRC Compressor Test Facility wherein the tests are conducted.

The major portion of this initial report comprises results from the preliminary calibration of the three-stage test compressor operated in the conventional configuration (i.e. with the stator rows stationary). This datum performance run was prematurely terminated by a drive train failure but some useful data were obtained at speeds up to about eighty percent of the design value. These data are compared with results from a previous series of tests on another compressor of the same aerodynamic design. The correlation of overall performance parameters was acceptable, but individual stage characteristics required considerable adjustment to obtain satisfactory agreement with previous results.

UNCLASSIFIED

1. Axial flow compressors - Test results
2. Compressor rotors
3. Turbofan engines
4. Gas Turbines
5. Turbomachinery

I. Chappell, M.S.
II. NRC, DME ME-234